Budker Institute of Nuclear Physics

Report on
Conceptual Design Study
of superconducting dipole magnet
Designed for CBM detector

Novosibirsk
May, 2017

THIS WORK HAS BEEN DONE UNDER SPECIFIC CONSULTANCY AGREEMENT BETWEEN FAIR FROM ONE SIDE AND BINP FROM THE OTHER SIDE FOR A FEASABILITY STUDY AND A CONCEPTUAL DESIGN OF A SUPERCONDUCTING DIPOLE MAGNET FOR THE CBM DETECTOR

Authors of the report are:

Mezentsev N.	e-mail: N.A.Mezentsev@inp.nsk.su
Bragin A.	e-mail: A.V.Bragin@inp.nsk.su
Pivovarov S.	e-mail: S.G.Pivovarov@inp.nsk.su
Shkaruba V.	e-mail: V.A.Shkaruba@inp.nsk.su
Erokhin A.	e-mail: A.I.Erokhin@inp.nsk.su
Khrushchev S.	e-mail: S.V.Khrushchev@inp.nsk.su
Tsukanov V.	e-mail: V.M.Tsukanov@inp.nsk.su
Volkov A.	e-mail: A.A.Volkov@inp.nsk.su
Tarasenko O.	e-mail: O.A.Tarasenko@inp.nsk.su
Syrovatin V	e-mail: V.M.Syrovatin@inp.nsk.su
Kholopov M.	e-mail: M.A.Kholopov@inp.nsk.su
Pyata E.	e-mail: E.E.Pyata@inp.nsk.su

Head of Laboratory,
Budker Institute of Nuclear Physics,
SB RAS, Novosibirsk, Russia

Mezentsev N.A.

CONTENT

1. Introduction

1.1 Content of the conceptual design

The scope of the contract is to design, manufacture, measure, deliver, install and commission the superconducting dipole magnet for CBM experiment at FAIR.

The Budker INP agrees to satisfy to the main parameters of the superconducting magnet for the CBM presented in "Collaboration Contract CBM Magnet BINP Annex3 specifications", design, prototyping, production, delivery, assembly and testing of the complete Dipole Magnet for the CBM experiment and tools necessary for its transport, storage and assembly Acceptance Test at the Customer's Site and Commissioning of the CBM superconducting magnet for the FAIR including extent of delivery, general conditions of the Contract, General mechanical requirements, general manufacturing standards, instrumentation and, documentation.

The conceptual design report should present the following items:

- Magnetic field calculations;
- Design of superconducting cable and coil;
- Quench calculations;
- Stress calculations, including all mechanical structures;
- Design of cryogenics including the cryostat, brunch box, feed box and cryogenic lines.

1.2 Preamble

The superconducting dipole magnet will be installed in the CBM detector at FAIR. The magnet provides a magnetic field integral of 1 T*m which is needed to obtain a momentum resolution of $\Delta p/p=1$ % for track reconstruction at FAIR beam energies.

The magnet gap has a height of 140 cm and a width of 250 cm in order to accommodate the STS with a polar angle acceptance of 25° and a horizontal acceptance of 30°. The magnet is of the H-type with a warm iron yoke/pole and cylindrical superconducting coils. The potted coil has 1749 turns. The wire – similar to the CMS wire – has Nb-Ti filaments embedded in a copper matrix with a total Cu/SC ratio of about 13 in the conductor. The operating current and the maximal magnetic field in the coils are 686 A and 3.25 T, respectively. The coil case made of stainless steel contains about 20 l of liquid helium for one coil. The vertical force in the coils is about 250 tons. The cold mass is suspended from the room temperature vacuum vessel by six suspension links. Six cylindrical support struts compensate the vertical forces. The energy stored in the magnet is about 5 MJ.

1.3 General requirements

The scope of delivery includes:

- Magnetic and engineering design of the magnet including all necessary tools, dimensioning calculations for stands and lifting units, etc;
- Engineering design of the Feed Box and the Branch Box incl. the cryogenic connection line;
- Production and delivery of the magnet (consisting of yoke, cold masses and cryostats, alignment components, Feed box and stand), the Branch Box, the cryogenic connection line and all tools;
- Engineering design, production and delivery of the Power Converter;
- Transportation of all components to site, complete assembly and the preparation of installation;
- Documentation.

1.4 General parameters

The following list contains the mandatory required parameters of the CBM dipole magnet:

Geometry

- Opening angle: ±25° vertically, ± 30° horizontally from the target
- Free aperture: 1.44 m vertically x 3.0 m horizontally, no conical geometry.

The Silicon Tracking System (STS) and its services will occupy all available space in the aperture, from left to right vertical yoke. It requires also space between lower coil and the vertical yoke bar, for detailed description see appendix in chapter 10. Distance target- magnet core end: 1m (STS detector must fit in).

- Total length: 1.5 m
- Free space upstream of the magnet: >2 m
- Field integral within STS detector (along straight lines): 0.972 Tm -> max. Field ≈ 1 T, depending on the magnet length
- Field integral variation over the whole opening angle along straight lines: ≤ 20% (± 10%)
- Fringe field downstream < reasonable value of the order of 50 to 100 Gauss at a distance of 1.6 m from the target at the position of the first RICH box (RICH only).

Operating conditions

- Operates at both polarities
- 100% duty cycle, 3 months/year, 20 years
- No real time restriction on the ramp: 1 hour up ramp
- Radiation damage (<10MG for organics): no problem
- Radiation Energy deposit in the cryogenic system: max. 1 W

Assembly

- Field clamps dismountable for MUCH
- Assembly in situ
- Weight restriction: crane 30 tons (including lifting jacks)
- Maximum floor load: 100 tons/m^2
- Beam height over magnet base: 2.7 m

Alignment

- Position accuracy: ± 0.2 mm
- Orientation accuracy (roll): ± 0.5 mrad

The requirements given above are mandatory.

2. General design

2.1 The magnet design

The conception of the total design of the CBM magnet is presented in the Fig. 1. It consists of the iron yoke, the superconducting magnet and the cryostat.

The iron yoke serves as a construction frame for the magnet and systems of the detector. Total mass of the iron yoke is about 140 tonnes. It has special tools for adjusting its position in all directions. The yoke is assembled of iron blocks having masses in the range between 3 and 13.6 tonnes. The material of the blocks is a kind of *steel 20* in Russian specification. The yoke blocks may have different magnet permeability, so they can be made of different steels, it will be discussed in the chapter of the magnetic field calculations.

The superconducting magnet is designed of two separated superconducting coils symmetrically placed in the detector close to the top and bottom blocks of the iron yoke. Such configuration represents a dipole magnet. The coils are placed around the taper blocks of the iron yoke which may be called as poles of the magnets. The distance between the poles is 1440 mm. Total view of the upper coil is shown on the Fig. 2.

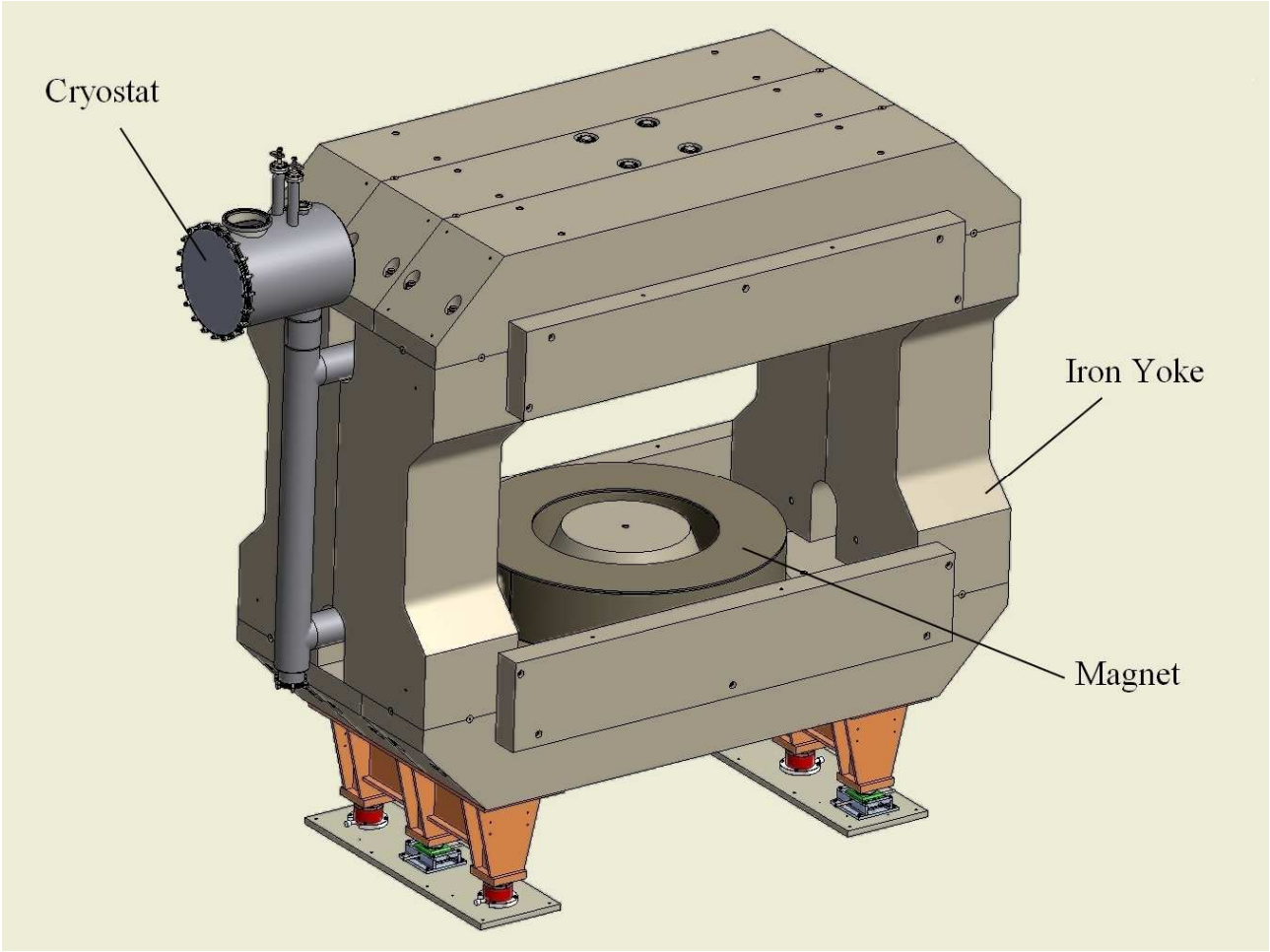

Fig. 1 Total view of the CBM magnet.

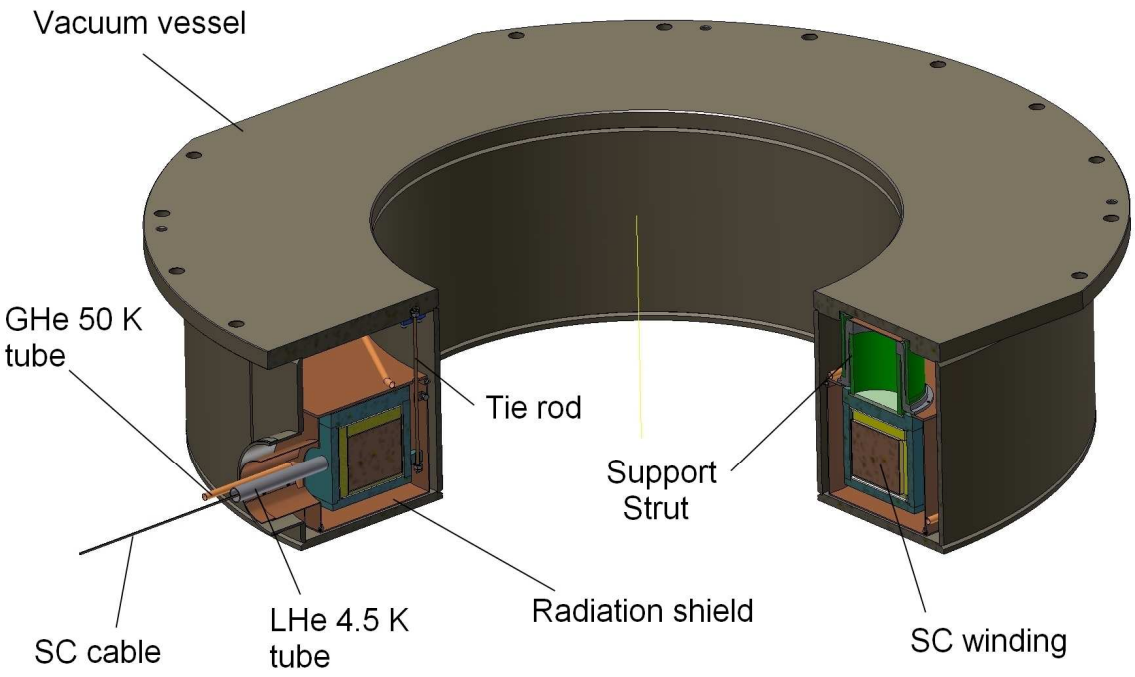

Fig. 2 Total view of the upper coil of the CBM magnet.

The superconducting winding is embedded in LHe case made of stainless steel. The LHe case is surrounded by copper radiation shield cooled by 50 K helium. This case should be covered by

aluminum foils in order to reduce its thermal emissivity. The radiation shields will be covered by multilayer insulation up to 20 layers. The coil is suspended inside the vacuum vessel on six struts. Six cylinder supports withstand attracting vertical force of the charged coils towards the taper iron.

The support struts design is shown on the Fig. 3. There are six support struts will be used. Each support should withstand compressive force up to 55 tonnes. They are consisted of cylinder composite and stainless steel (a kind of 316LN is preferable on yield strength) coaxial tubes. The material of the composite is a kind of G-10. They will give major part of the heat loads on the cryogenic system. The hot spots on the LHe case should be taken into account in the design. It will be also important to reduce emissivity of the composite cylinder by gluing aluminized Mylar foils.

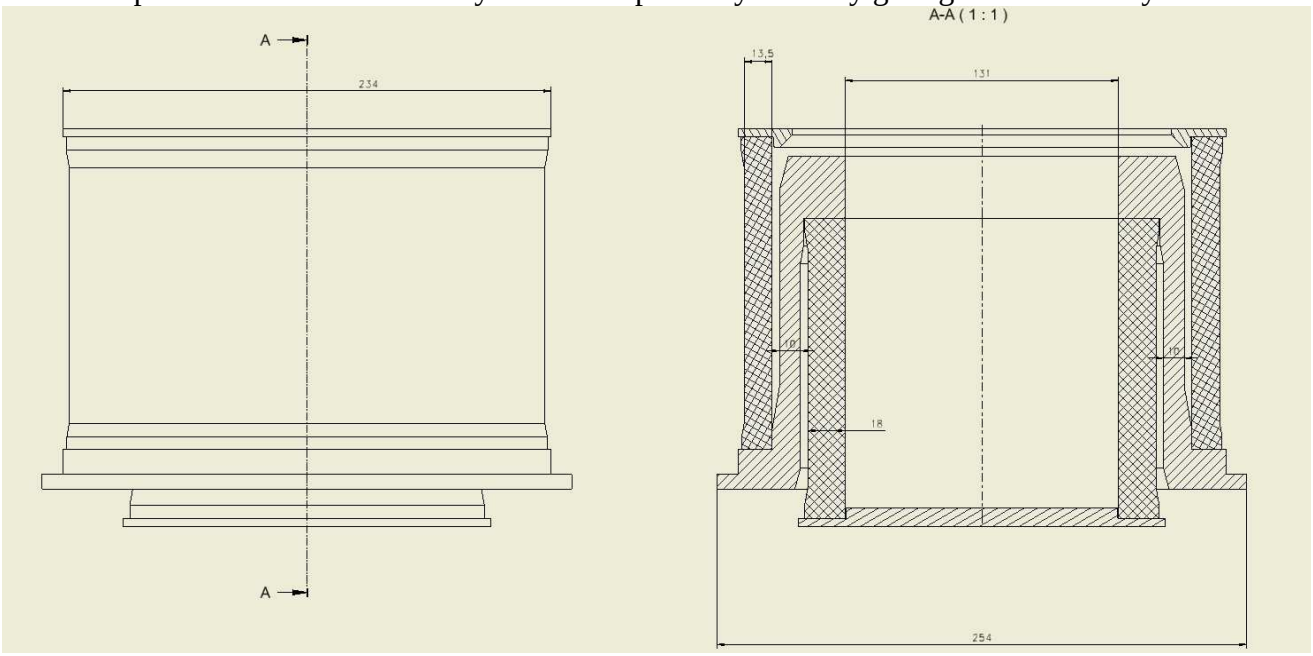

Fig. 3. View of the support struts. It consists of two G-10 cylinders and one cylinder of stainless steel.

2.2 Superconducting coil design

The total view of the superconducting coil as a cold mass at 4.5 K is shown on the Fig. 4. The parameters of the superconducting winding are listed in the Table 1.

The winding will be made of two pieces of the superconducting cable having length of about 4.5÷5 km. One splicing will be made during a winding procedure using soft soldering on a base of PbSn alloy. The splicing place will be positioned on the opposite site of the winding with respect to the winding site touching the LHe case where the support dimples are made. Now it is discussed to make dry winding in special winding tools, after this the coil winding will be impregnated by epoxy resin separately from the LHe case as proposed in the TDR. Fine powder of Al_2O_3 is often added to epoxy resin that improves thermal parameters of epoxy compound. Such technology is widely used in BINP.

The LHe case made of 316LN stainless steel is designed to withstand large vertical forces from the charged coils and from internal pressure during a quench. The thickness of the walls of this LHe case is from 20 to 30 mm. The yield strength of 316LN at 77 K is 1400 MPa [Iwasa, p. 638].

The flow of 4.5 K liquid helium in the LHe case is schematically shown on the Fig. 6. Liquid helium should enter the case via one tube and exit via another. It will be made a wall of G-10 composite to prevent immediate flow of liquid helium from one tube to another around the welding place of these tubes to the LHe case. These tubes will be placed differently for upper and lower coils of the magnet in such a way that the exit tube should be placed at highest position in the LHe case. In this case most part of gaseous helium will exit the LHe volume. Accumulation of gaseous

helium especially in the upper coil is very undesirable because it will increase temperature in the hot spots around the support struts. Heat transfer coefficient for gaseous helium is at least 10 times lower than for pool boiling liquid helium.

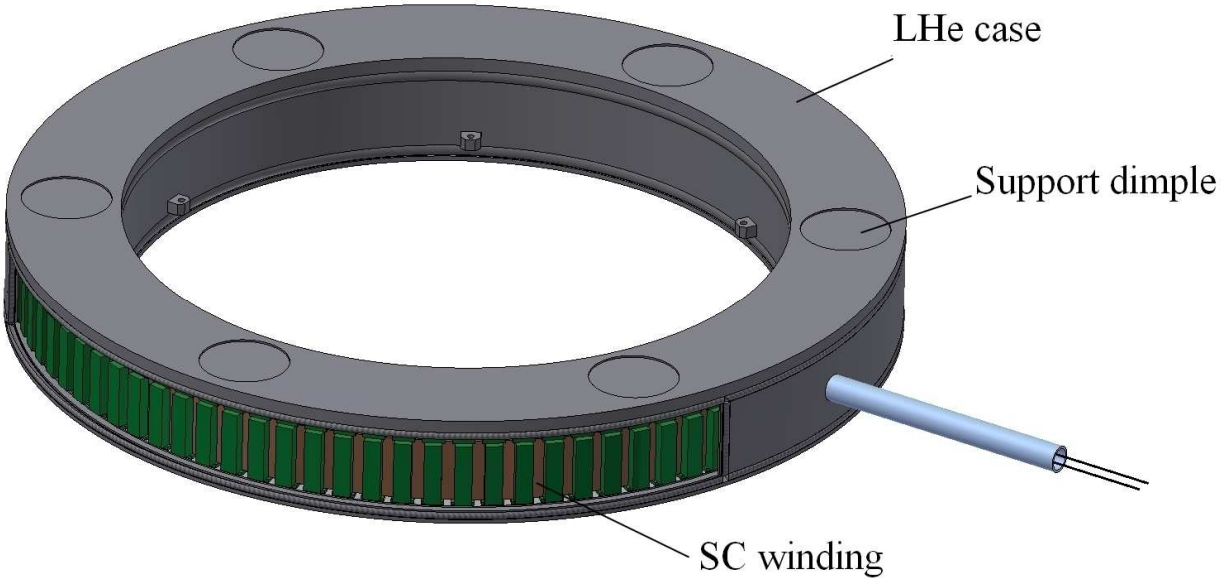

Fig. 4 The superconducting coil in the LHe case.

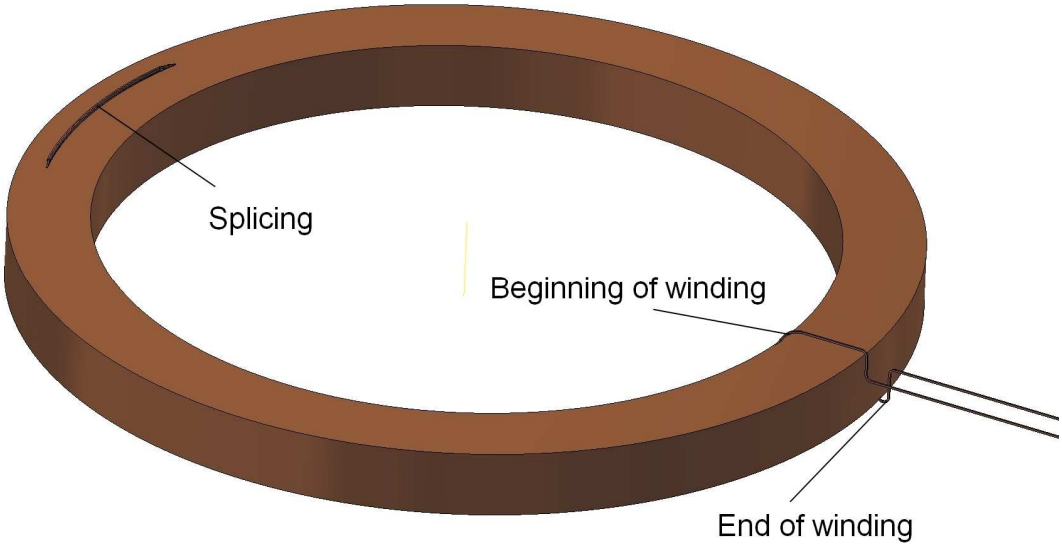

Fig. 5. Design of the CBM coil winding.

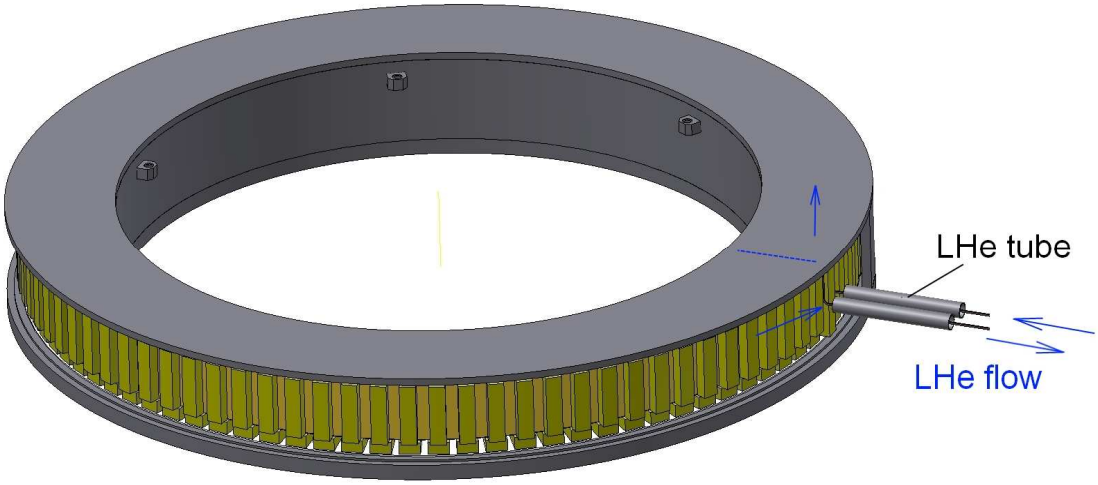

Fig. 6. Schematic view of liquid helium flow in the LHe case of the coil.

Table 1 Superconducting winding parameters

Coils parameters	**Values**
Inner radius of the winding, mm	1390
Cross section sizes of the winding:	
height, mm	131
radial length, mm	158
Number of turns in one coil	1754
Number of layers in one coil	53
Interlayer insulation, mm	0.3
Operating current Io, A	686
Test current, Io*1.2, A	823
Magnetic field on the coil Bmax, T	3.25
Io/Ic ratio along the load line, %	52
Io/Ic at fixed B, %	25
Operating temperature, K	4.5
Temperature of current sharing, K	6.84
Stored energy of the magnet, MJ	5.1
Stored energy of the magnet at the test current, MJ	6.4
Cold mass of one coil at 4.5 K, kg	1800
Cold mass of one winding, kg	790
Inductance of the magnet at full current, H	21.2
E/M ratio for two windings, kJ/kg	3.2
Mutual inductance between the coils, H	0.21
Vertical force on one coil toward the yoke, MN	2.6 (2.8 if only one coil charged)
Vertical force on one coil toward the yoke at the test current, MN	3.3 (3.5 if only one coil charged)

The parameters of the superconducting cable are the same which were specified in the TDR except the cable length, see Table 2. BINP proposes to make superconducting winding of two pieces as stated above. It will give more convenience as in producing the cable for BINP subcontractors as in manufacturing of the superconducting coil.

The superconducting cable will be produced of NbTi/Cu wire of ∅1.2 mm by co-extrusion into

a copper matrix to have high Cu/NbTi ratio as it is shown on the Fig. 7. Working point is shown on the load line for the CBM magnet, it corresponds the 3.25 T of magnetic field, see Fig. 8. The I_o/I_c ratio and other critical parameters of the wire are the same that were proposed in the TDR.

Table 2 Superconducting cable parameters approved by manufacturers in May 2017

SC wire parameters	**Values**
Rectangular bare/insulated sizes:	
a, mm	2.02/2.62
b, mm	3.25/3.85
facets radius, mm	0.45
Cable total length, km	8.6
One piece of the cable length, km	5
Cu/NbTi ratio	>9.1
RRR	>100
Filament diameter, μm	37±1
Number of filaments	620
Filament twist pitch, mm	<45
Cu+NbTi cross section area, mm^2	6.342
NbTi cross section area, mm^2	<0.628
I_c (5 T, 4.2 K), min A/	1754
I_c (4.5 K, 3.3 T), min A	2358

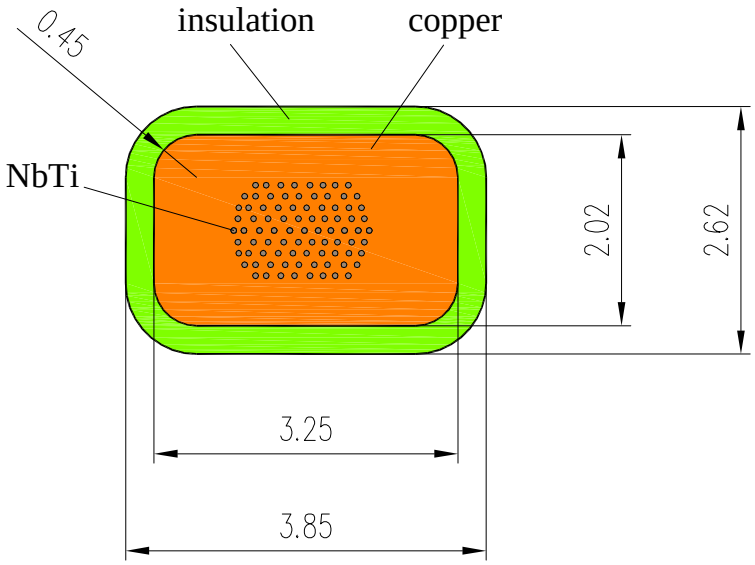

Fig. 7 Cross section of the proposed SC wire for the CBM magnet.

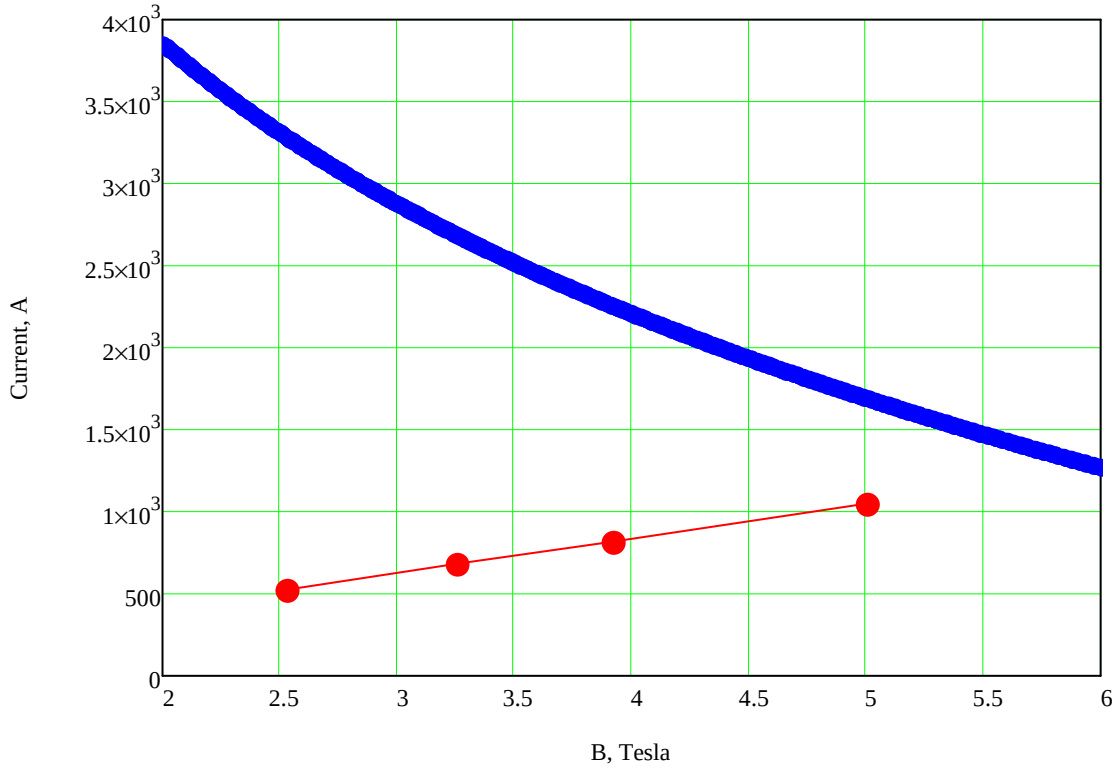

Fig. 8. Load line of the CBM magnet at 4.5 K.

2.3 Cryostat design

The CBM magnet will be supplied from external cryogenic station with helium of 4.6 K at 3 bar and helium of 50 K at 18 bar. The magnet itself will be filled with liquid helium from the cryostat placed on the top of the iron yoke as shown on the Fig. 1. The design of the cryostat is shown on the Fig. 9. The volume of the liquid helium will be about 40 l. The level of liquid helium will be controlled to contain about 20 l of liquid helium. The LHe volume will be filled from the Feed Box via the phase separator.

The cryostat also has ports for vacuum measurement and initial pumping of the magnet and the Feed Box.

The current leads are designed for the current up to 1 kA. Some part of the gaseous helium entering the cryostat will cool these current leads. If additional gas will be needed then a heater may be installed.

The neck of the cryostat serves for various purposes. On the warm part of a rapture diaphragm, valves for connection with multipurpose line, connections for measurements and filling of liquid helium in the BINP tests will be placed.

The radiation shield of the cryostat will be cooled by return line of the gaseous helium at about 55 K of temperature. The direct line of 50 K helium should directly go to the magnet for cooling its supports and the radiation shields.

The radiation shield of the cryostat will be suspended on ball supports made of a kind of G-10 composite. The outer surfaces of the shield will be covered by multilayer superinsulation. .

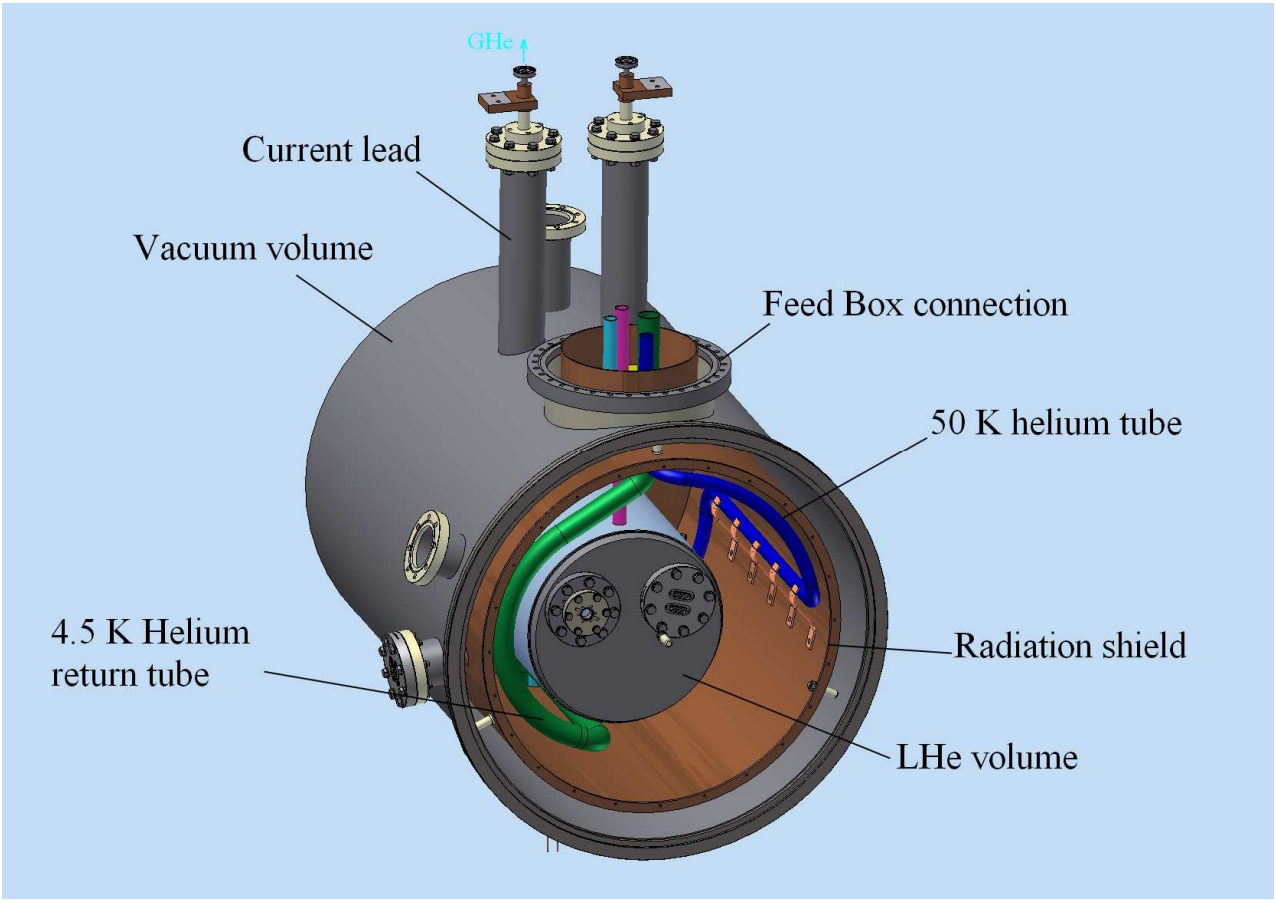

Fig. 9. View of the cryostat top of the CBM magnet.

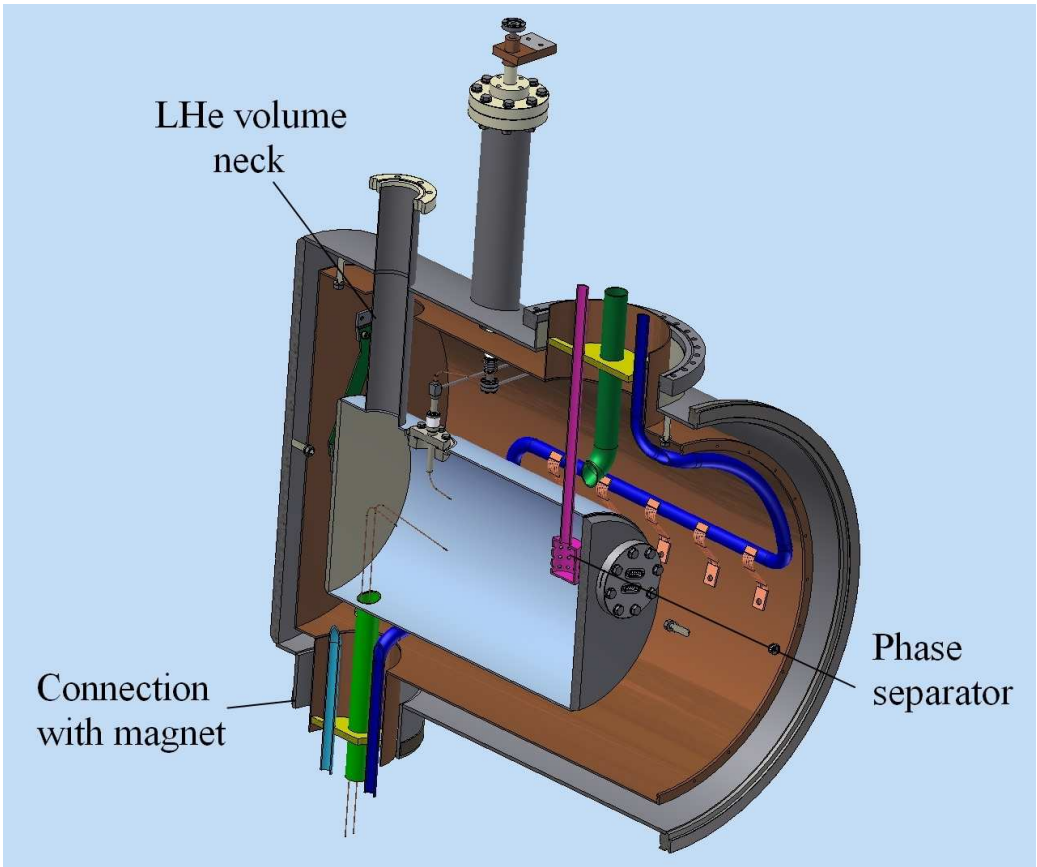

Fig. 10. Cross section of the cryostat.

3. Design calculations

3.1 Magnetic field calculations

The magnetic field calculations should present that the general design of the magnet gives the desired parameters of the magnetic field listed in the specifications, and results of forces acting on the yoke blocks and the magnet.

The 3D calculations were made in COMSOL code, 2D calculation in ANSYS. The iron yoke steel was chosen as Steel1010 (as Russian specification, that corresponds to Steel 1020 of USA and Steel 1.0402 of Germany). The taper part of the yoke is a kind of ARMCO Steel or Steel 08kp (as of Russian specification, which corresponds to Steel 1008 of USA and Steel 1.0322 of Germany).

.

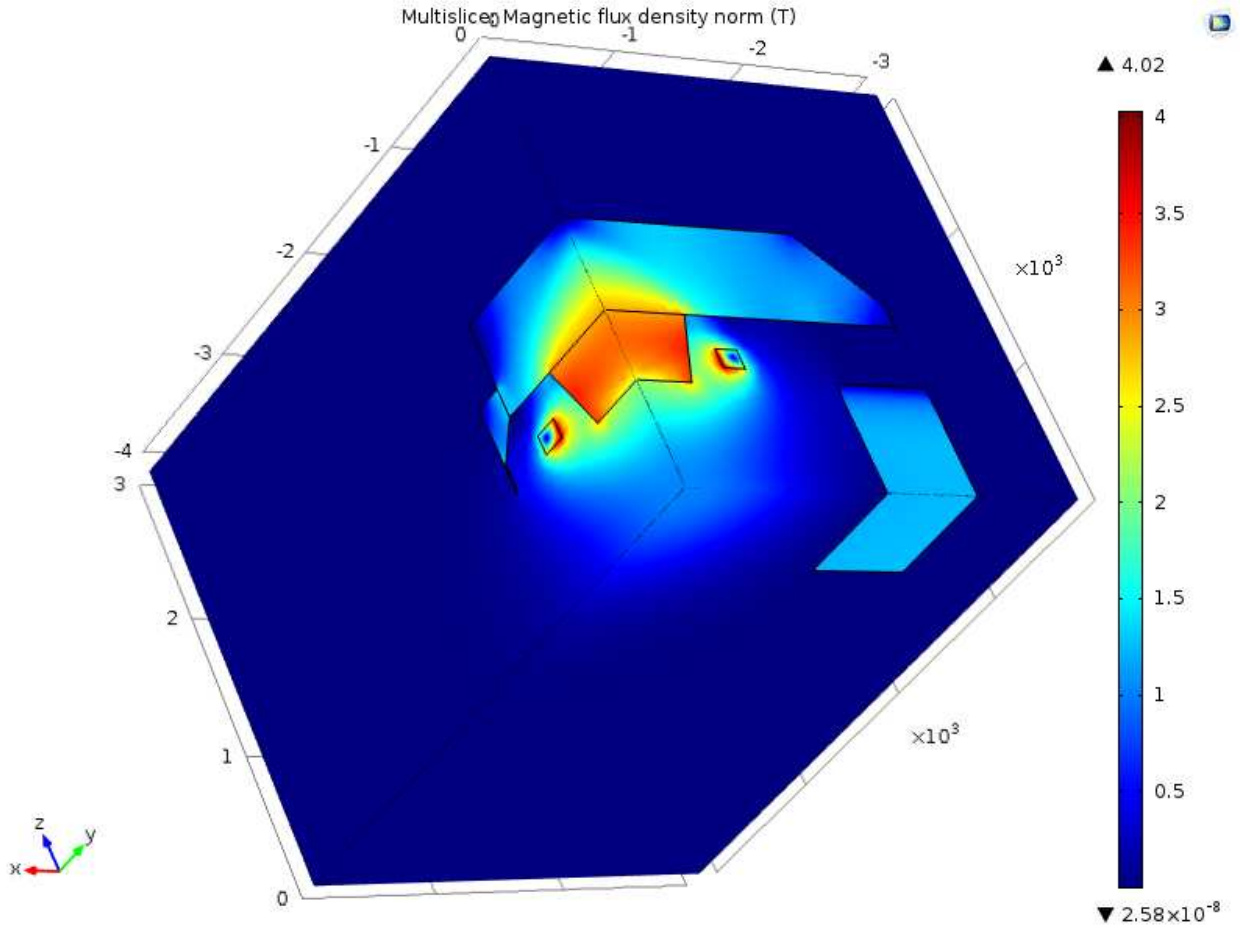

Fig. 11. Magnetic field distribution in the 3D model.

The magnetic field distribution along the central line of the detector is shown on the Fig. 12. The integral from the target along the central line is 0.886 T*m in the length of 1 m.

The forces on the coils and the taper iron were calculated in the ANSYS 2 D model. The accuracy of the values of the forces is about 5% that is according to calculations in the TDR.

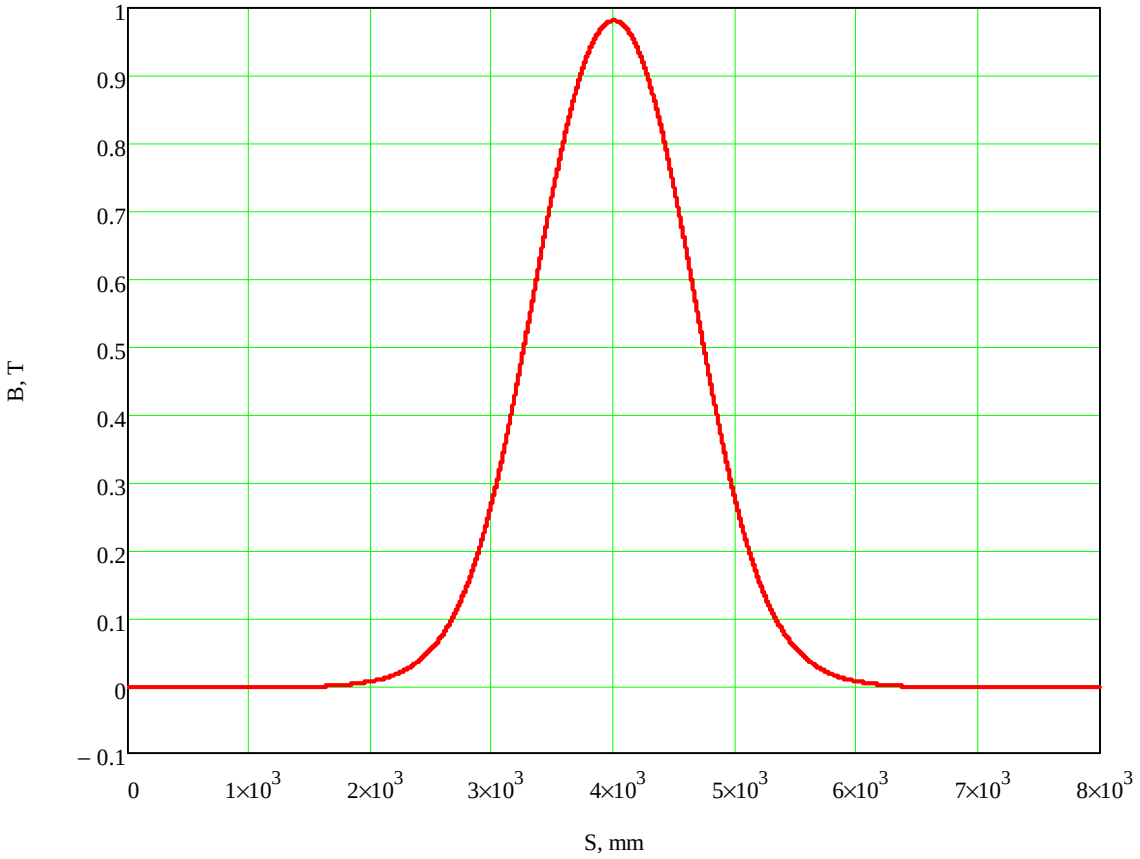

Fig. 12. Magnetic field distribution along the line from the center of the magnet detector. The integral in the vicinity of the center along the line ± 0.5 m is 0.895 T*m.

Results of the magnetic field calculation:

- influence of different steels having various permeability is shown;
- Vertical force on one coil toward the yoke is 2.6 (2.8 if only one coil charged) MN and is 3.3 (3.5 if only one coil charged) MN;
- force on the iron tapers is about 300 t at 686A toward the center of the detector, and about 370 t at test current;

3.2. Mechanical calculations

The mechanical calculations of this CDR include:

- deformation of the iron yoke after allied force from attracting taper iron parts to the center of the magnet, Fig. 13, Fig. 14;
- influence of buckling atmosphere pressure on the vacuum case of the coil, Fig. 15 and Fig. 16;
- results of internal pressure up to 20 bar at room temperature inside the coils stainless steel case, Fig. 17 and Fig. 18;
- results of compressive force on the support struts,

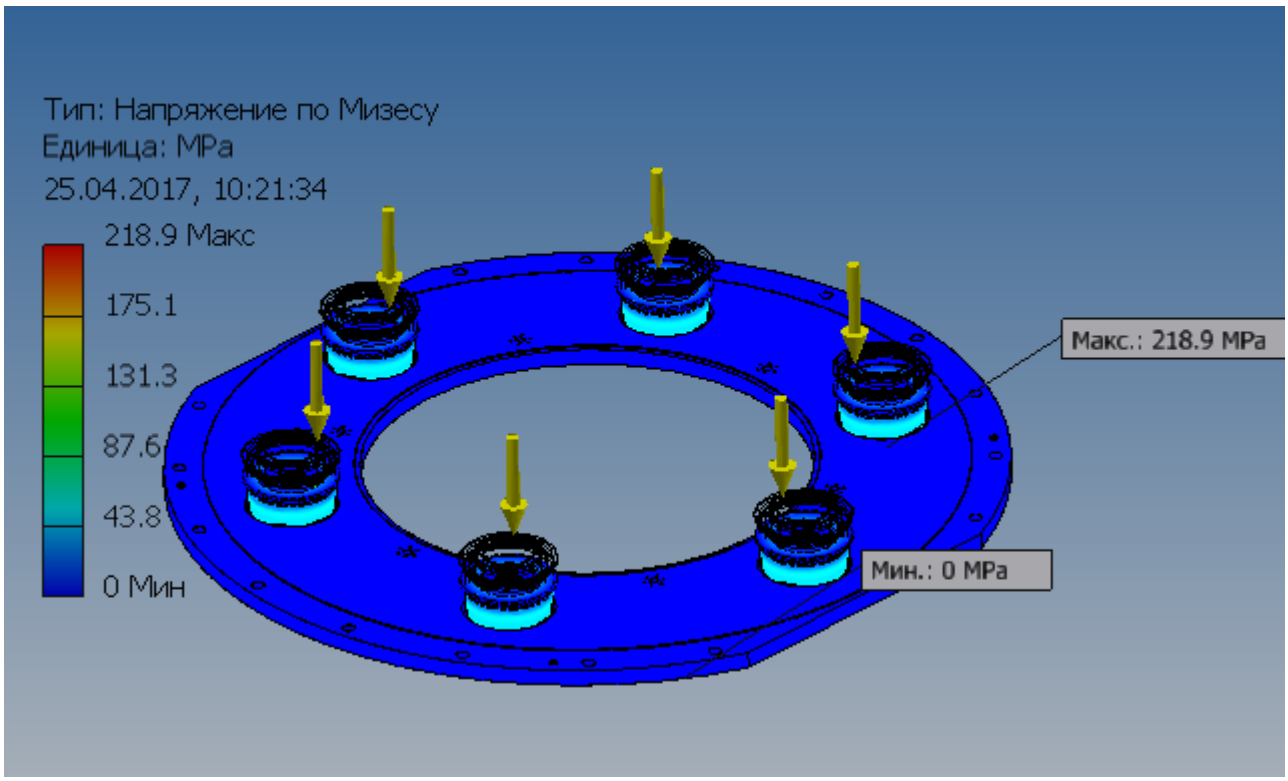

Fig. 19 and Fig. 20;
-

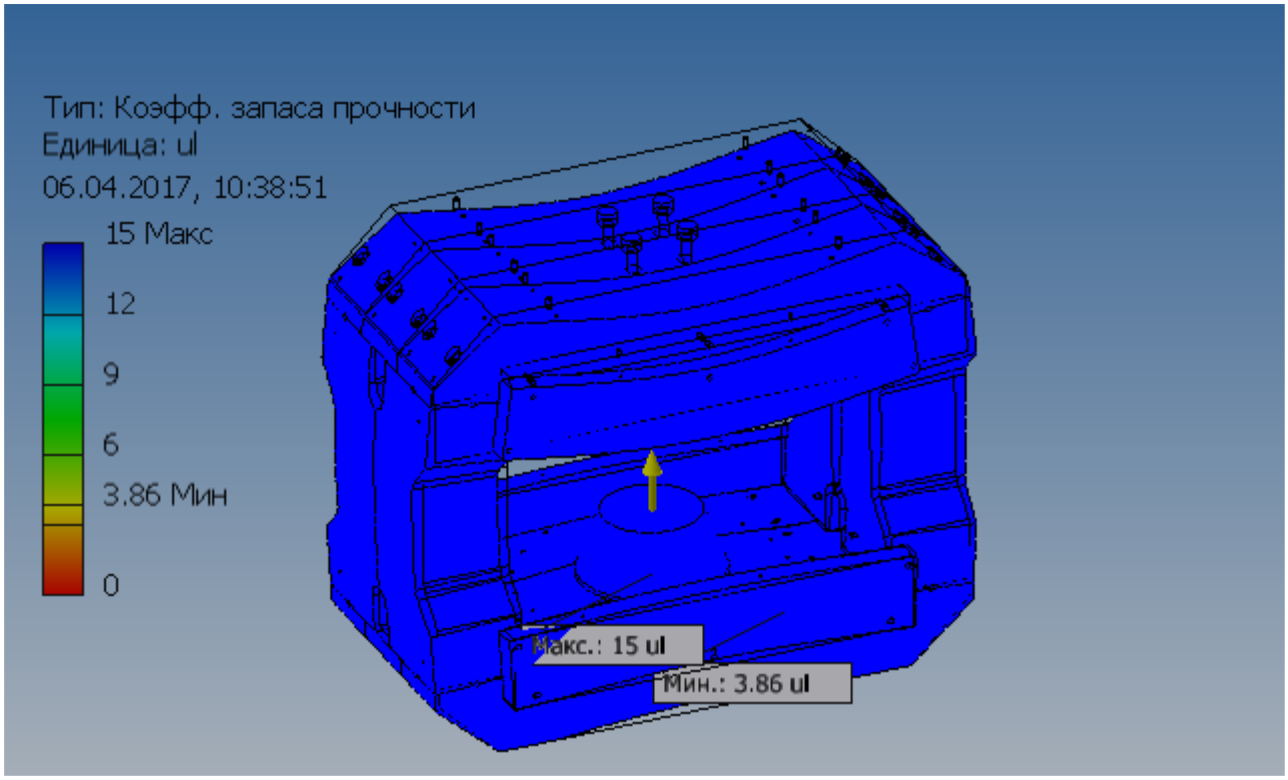

Fig. 13. Deformation of the iron yoke from the force on the taper iron without back force from the coil (worse case).

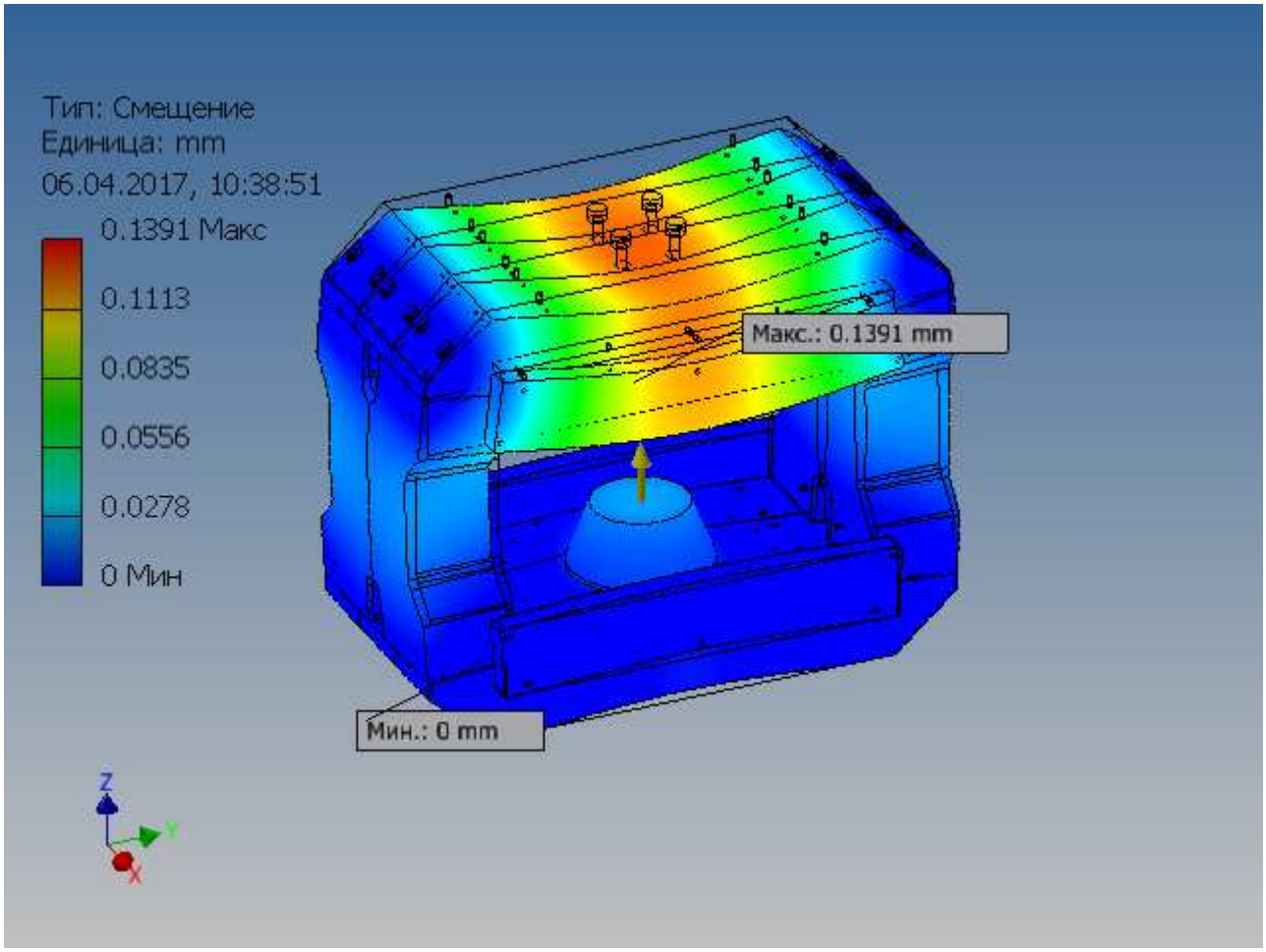

Fig. 14. Deformation of the iron yoke from the force on the taper iron without back force from the coil (worse case). The maximal deformation is 0.14 mm.

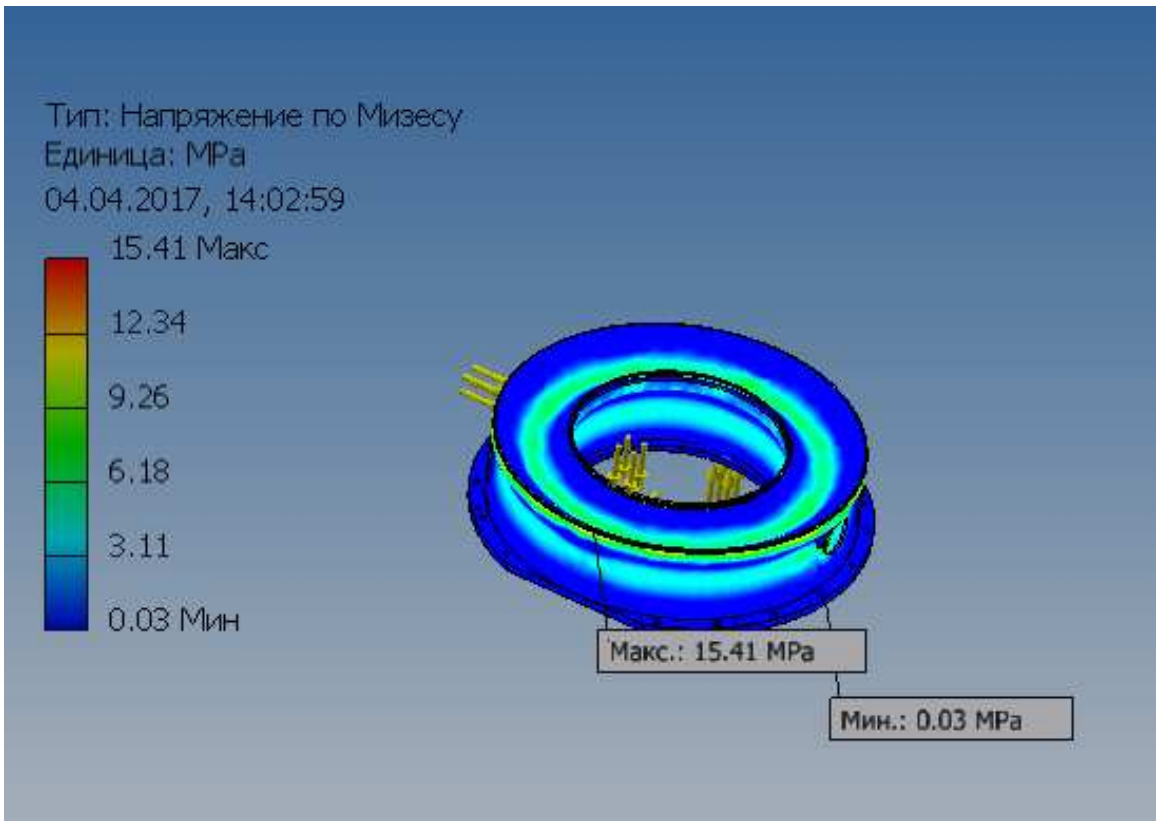

Fig. 15 Influence of buckling atmosphere pressure on the vacuum case of the coil – von Mises stress in MPa.

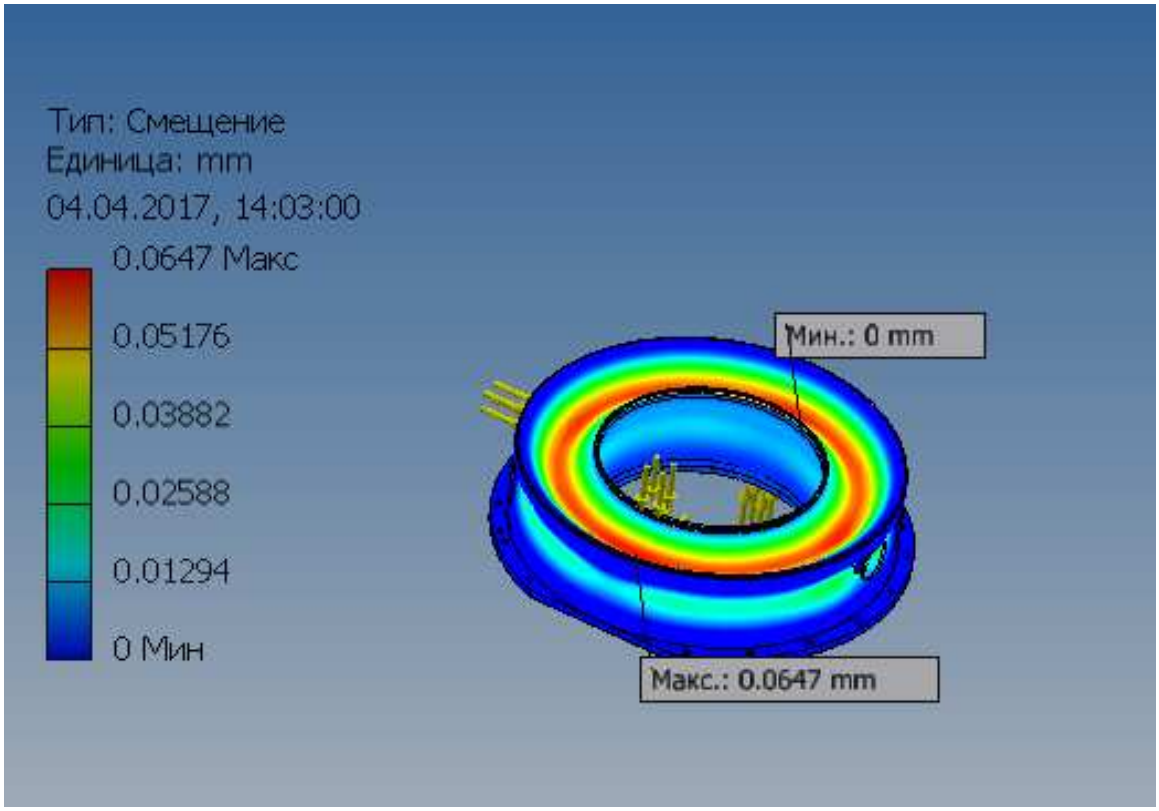

Fig. 16. Influence of buckling atmosphere pressure on the vacuum case of the coil – deformation, mm. Maximal deformation is 0.0647 mm.

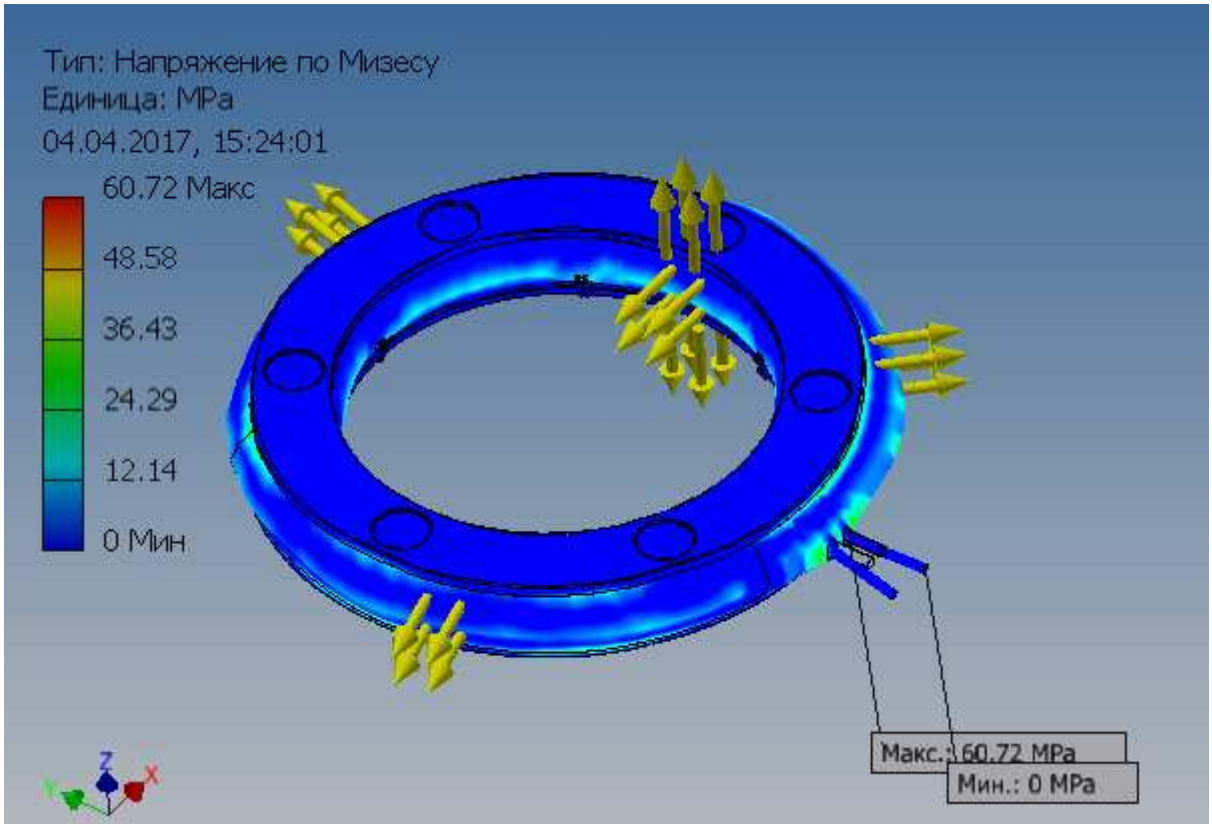

Fig. 17. Result of internal pressure increasing up to 20 bar – von Mises stress

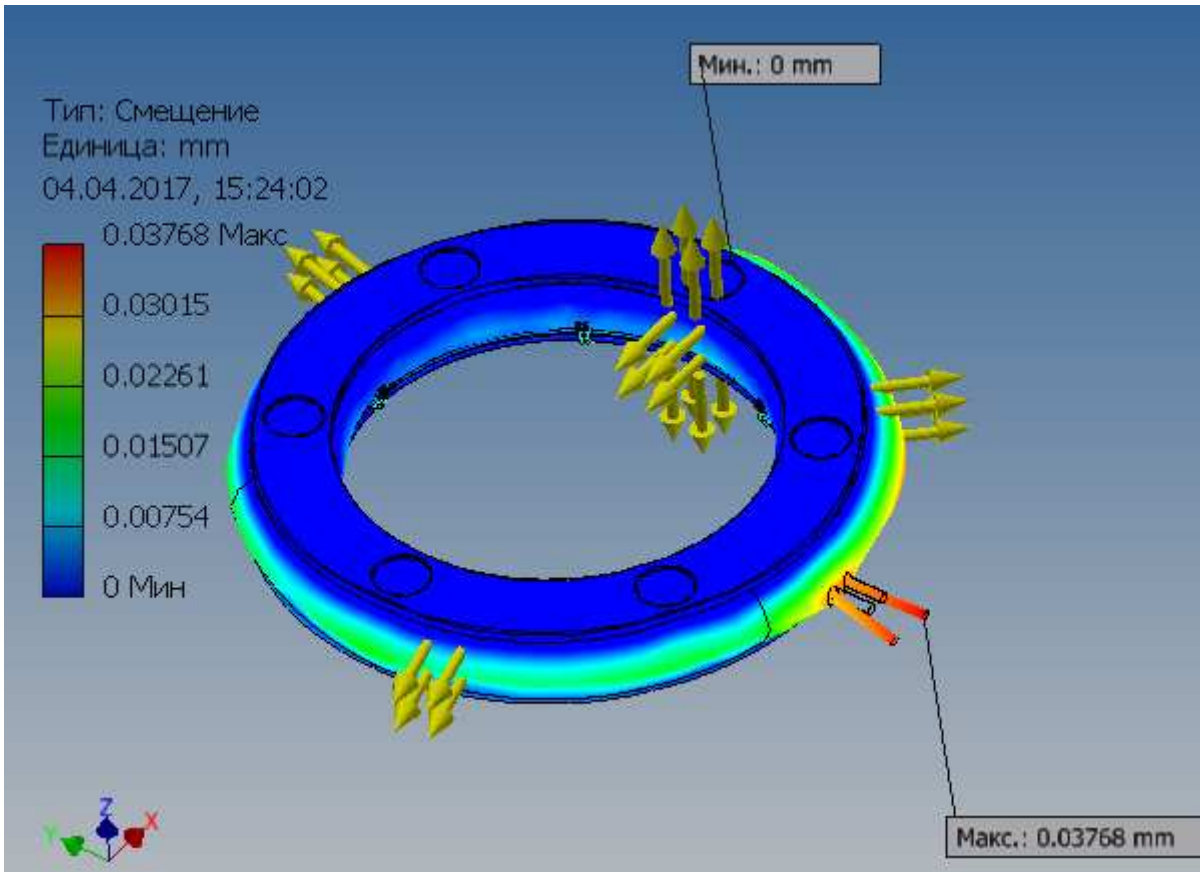

Fig. 18. Result of internal pressure increasing up to 20 bar – deformation in mm.

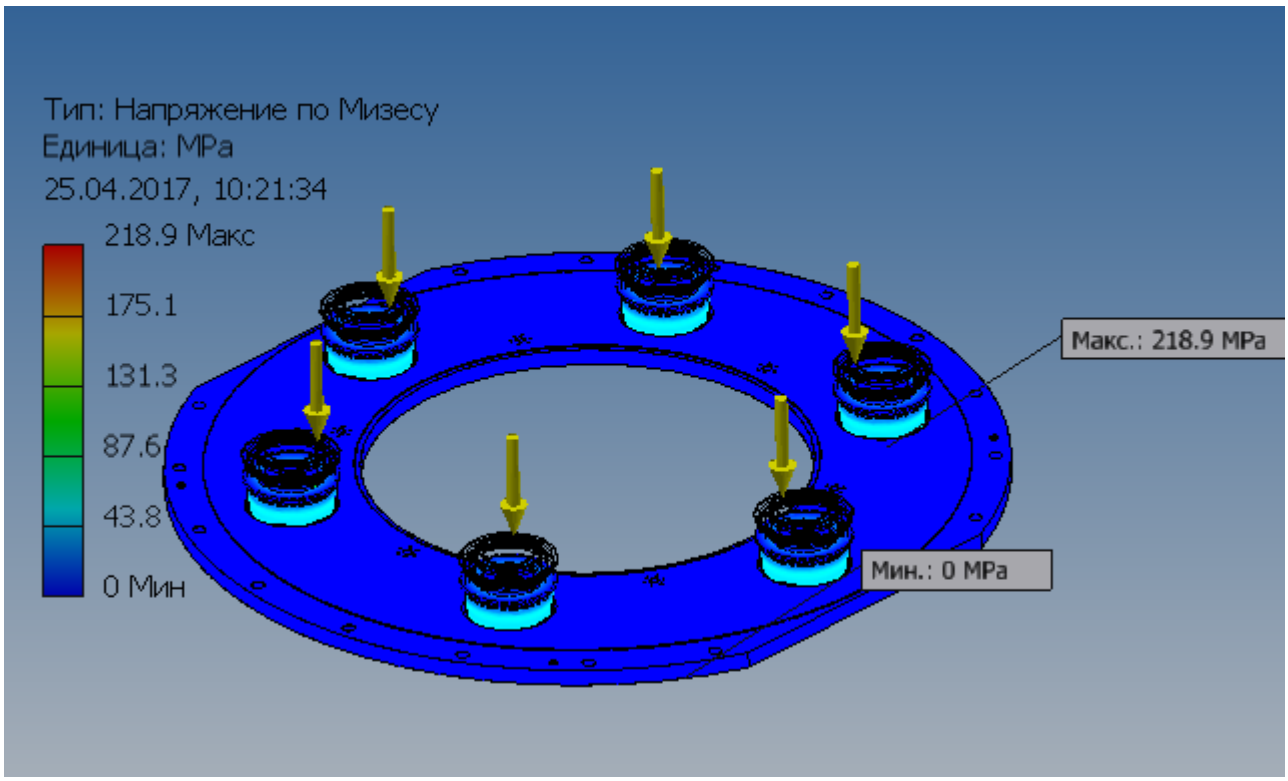

Fig. 19. Von Mises stress in the support struts at application of 3 MN vertical force. The maximal stress is in the stainless steel cylinder of the support which is 219 MPa.

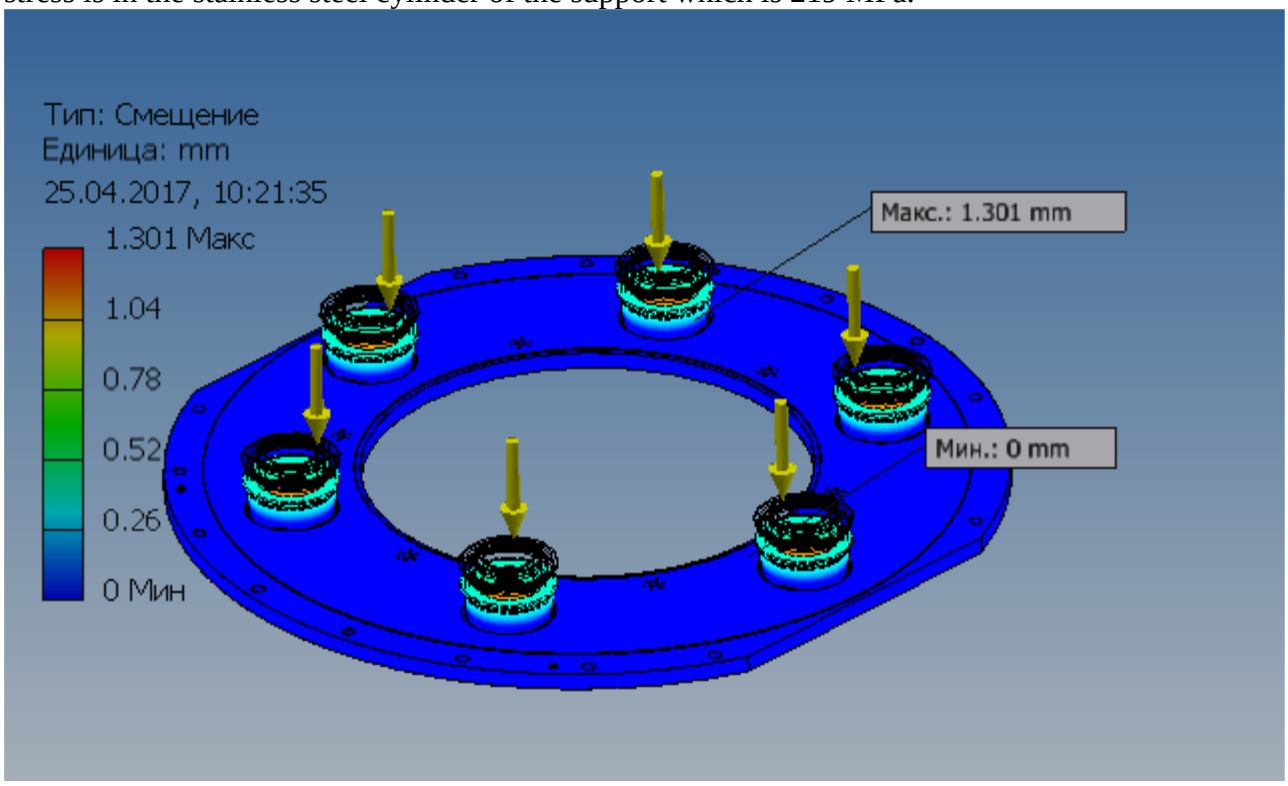

Fig. 20. Support displacement after application of 3MN of the vertical force.

Buckling forces on the supports:

$F_{cr} = C \cdot \frac{\pi^2}{L^2} \cdot E \cdot J$, where C – coefficient depending on the fixation of the ends of a beam, L –

length of a beam, E – Young modulus, J= $\frac{\pi}{64}(d_1^4 - d_2^4)$ - radial inertia momentum of the hollow cylinder.

3.3. Heat load estimations

The results of the heat loads estimations are presented in the tables below.

Estimations of the heat loads to 4.5 K helium

The thermal radiation on the LHe coil cases was estimated as:

$Q = \varepsilon S \sigma T^4$, where ε - total emissivity was taken as 0.02, S – surface area of the LHe case is 4.2 m^2, T – radiation shield temperature was taken as 60 K.

The heat load from the support struts for G-10 elements was estimated as:

$Q = \lambda S^* \Delta T/L$, where λ - thermal conductivity was taken as 0.3 W/(m*K), S – cross-section area is about 9.1^*10^{-3} m^2, ΔT – temperature difference was taken as 60 K, L – length is about 0.16 m.

The heat load from the tie rods was estimated as:

$Q = \lambda S^* \Delta T/L$, where λ - thermal conductivity was taken as 0.15 W/(m*K), S – cross-section area is about 1.1^*10^{-4} m^2, ΔT – temperature difference was taken as 60 K, L – length is about 0.25 m.

Joule heat in the soldered splices was estimated for soldering on 5 cm of length and resistance will be about 5^*10^{-8} Ohm and at 686 A of current.

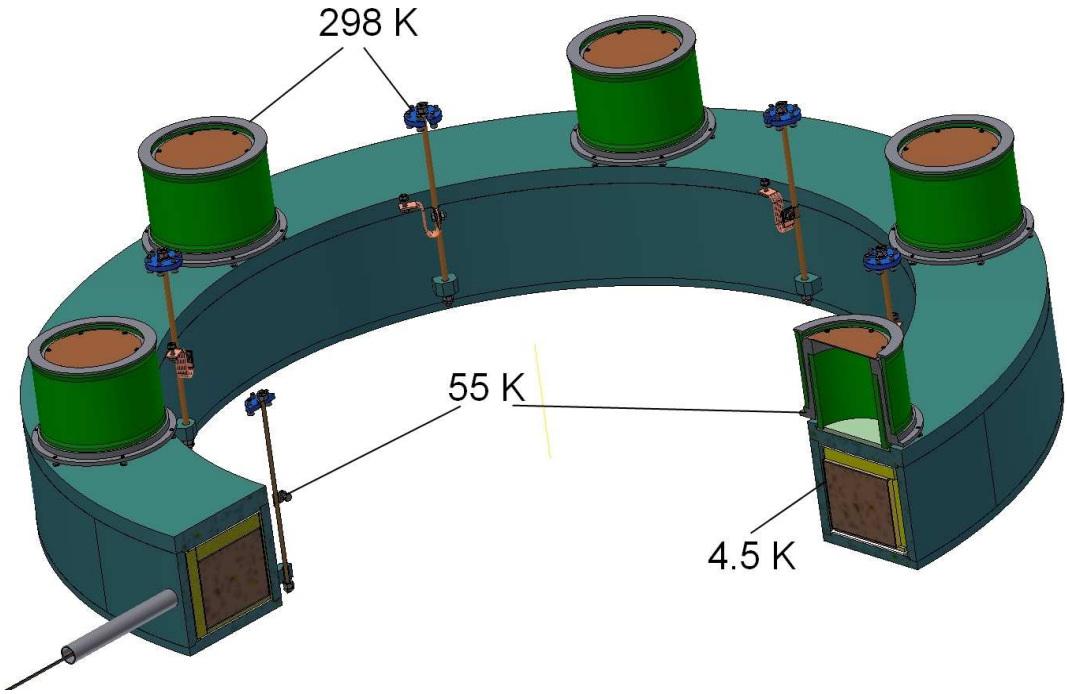

Fig. 21. View of the cold mass of the magnet connected by tie rods and support struts to the vacuum vessel.

Table 3 Heat loads on 4.5 K helium from both coils and the cryostat

Heat load from	**Values**
Thermal radiation on the LHe case, W	0.12
Support struts, W	13
Tie rods, W	0.05
Soldering connection of the cable (at least 6 short splices), W	0.12
Thermal radiation on the cryostat, W	0.015

Cryostat suspension, W	<0.1
Current leads, W	0.5
Measurements wires, W	<0.1
Heat bridges of the cryostat neck and others connections, W	<0.1
Total, W	***~ 14.1***

Hot spot by the support struts

The support struts give largest part of the magnet heat loads. The superconducting winding will press the LHe case exactly opposite these struts. ANSYS calculations were made to see the possible hot spots in these places on the LHe case. The results of the calculations are shown on the Fig. 22 and Fig. 23. The model is of axial symmetry along Y axis. The bottom is the stainless steel case cooled by helium of 4.5 K temperature. The model is worse case with respect to 3D model because the heat flow goes only in one direction, i.e. less area of LHe case cooled by liquid helium is taken in the 2D model. Two temperatures were fixed: 295 K at the top of the support and 55 K at the place of the thermal connection with the radiation shield of the magnet.

The temperature distribution in the Fig. 22 is when the LHe case is cooled by helium at 1 kW/(m^2*K) of the heat transfer coefficient that respects to a nucleate boiling condition in large volume.

The temperature distribution in the Fig. 23 is when the LHe case is cooled by helium at 30 W/(m^2*K) of the heat transfer coefficient that respects to cooling by gaseous helium at natural conditions. The effect of the copper foil not cooled by LHe placed between the LHe case and the spacers is shown on the Fig. 24.

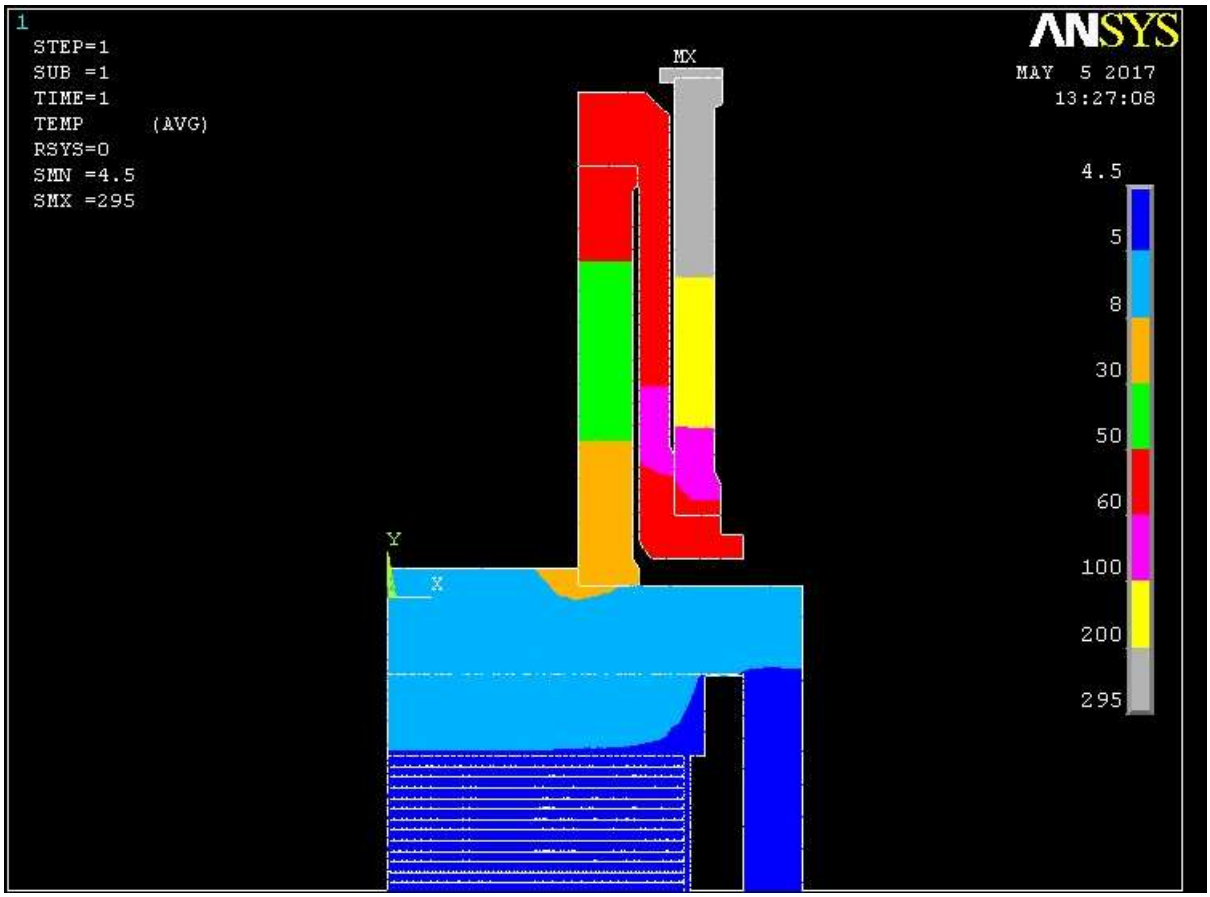

Fig. 22. Temperature distribution in the support struts at bulk temperature of 4.5 K and the heat transfer coefficient of 1 kW/(m^2*K).

Fig. 23. Temperature distribution in the support struts at bulk temperature of 4.5 K and the heat transfer coefficient of 30 W/(m^2*K).

Fig. 24. Temperature distribution in the support struts at bulk temperature of 4.5 K and the heat transfer coefficient of 30 W/(m^2*K). The copper foil of 1 mm thickness is placed between the winding and the G-10 spacers.

Estimations of the heat loads to 50 K helium

The thermal radiation from the vacuum vessel on the radiation shields covered by multilayer insulation may be estimated as:

$Q = q*S$, where, S – surface area of the shields is ~ 5 m^2, q – experimentally determined heat flux, its typical value is about 1 W/m^2.

The heat load from the support struts for G-10 elements was estimated as:

$Q = \lambda S*\Delta T/L$, where λ - thermal conductivity was taken as 0.5 W/(m*K), S – cross-section area of one support strut is about $9.1*10^{-3}$ m^2, ΔT – temperature difference was taken as 220 K, L – length is about 0.16 m.

The heat load from the tie rods was estimated as:

$Q = \lambda S*\Delta T/L$, where λ - thermal conductivity was taken as 0.15 W/(m*K), S – cross-section area is about $1.1*10^{-4}$ m^2, ΔT – temperature difference was taken as 220 K, L – length is about 2*0.15 m (two cylinders).

Table 4 Heat loads on 50 K helium from both coils and the cryostat

Heat load from	**Values**
Thermal radiation on the shields from the vacuum vessel, W	10
Support struts, W	38
Tie rods, W	0.5
Thermal radiation on the cryostat shield, W	1.5
Cryostat suspension, W	2
Current leads, W	50*
Measurements wires, W	0.5
Heat bridges of the cryostat neck and others connections, W	1
Total, W	~ 104

*) It will be corrected after detailed design of the current leads

The estimation of heat loads from on the Branch Box, the Feed Box and on the transfer line are presented in the Table 5 and Table 6.

The thermal radiation on the surfaces at 4.5-4.6 K was estimated as:

$Q = \varepsilon S\sigma T^4$, where ε - total emissivity was taken as 0.03, S – surface area of the BB, FB and the transfer lines surfaces at 4.5 K is about 7 m^2, T – radiation shield temperature was taken as 60 K.

The heat load from the control valves was estimated on example of Weka valves of DN15 size as:

$Q = N*Q_v$, where N – is the number of valves, in our case is 19, Q_v – the heat load from one valve specified by manufacturer, which is in our case about 0.8 W.

The heat load from the check valves was estimated as:

$Q = \lambda S*\Delta T/L$, where λ - thermal conductivity of stainless steel tubes and bellows was taken average as 3 W/(m*K), S – cross-section area is about 10^{-3} m^2, ΔT – temperature difference was taken as 60 K, L – length is about 0.2 m.

Table 5 Heat loads on 4.6 K helium from the Branch Box, the Feed Box and the transfer line

Heat load from	**Values**
Thermal radiation on 4.5 K surfaces from the shields on the FB and BB, W	0.15
Supports and suspensions, W	< 2
Control Valves, W	15.2
Check Valves, W	0.9
Measurement wires, W	< 0.01
Heat bridges of the cryostat neck and others connections, W	< 1

Total, W	19.26

The thermal radiation from the vacuum vessel on the radiation shields covered by multilayer insulation may be estimated as:

Q = q*S, where, S – surface area of the shields is ~ 7 m^2, q – experimentally determined heat flux from room temperature via multilayer insulation, its typical value is about 1 W/m^2.

The heat load from the check valves was estimated as:

Q = λS*ΔT/L, where λ - thermal conductivity of stainless steel tubes and bellows was taken average as 10 W/(m*K), S – cross-section area is about 10^{-3} m^2, ΔT – temperature difference was taken as 220 K, L – length is about 0.2 m.

Table 6 Heat loads on the 60 K helium (return line) from the Branch Box, the Feed Box and the transfer line

Heat load from	**Values**
Thermal radiation on the shields from the vacuum vessel, W	7
Support and suspensions, W	20
Control valves, W	38
Check valves, W	11
Measurement wires, W	< 1
Heat bridges of the cryostat neck and others connections, W	5
Total, W	82

As a conclusion, total heat load for the CBM detector:

for 4.6 K helium is Q = 33.4 W; for 50 K helium is Q = 186 W;

The mass rates at normal operation are G = Q/Δh:

G = 1.7 g/s for 4.6 K helium;

G = 1.8 g/s for 50 K helium which is heated from 50 to 69 K, Δh = 105 J/g. Some part of this rate will be excluded for the current leads cooling. In further estimations it will be assumed that all of 1.8 g/s will go through the return cooling line.

3.4 Quench calculations

The quench analysis evaluates behavior of the superconducting coils during a quench to give maximal temperature in the hot spot, voltage inside the winding, etc.

Its worth to evaluate *stability parameters* of the CBM coils prior the quench estimations, they allow to see the impact the big amount of the copper stabilizer in the SC wire.

The minimal length of the normal zone propagation in a SC wire is

$L = \sqrt{\frac{2\lambda(T_c - T_o)}{\rho J_c^2}}$, where λ - thermal conductivity coefficient of the copper matrix, ρ - electrical resistivity of the copper, Jc – current density, Tc and To – critical and operation temperature of the wire.

$L = \sqrt{\frac{2 \cdot 400 \cdot 4}{10^{-10} \cdot 7.7^2 \cdot 10^{14}}} = 0.073$ m.

Minimal energy for the normal zone propagation:

$E = C\gamma A T_{av} \sqrt{\frac{2\lambda(T_c - T_o)}{\rho J_c^2}}$, where Cγ - heat capacity [J/(kg*K)], A – cross-section area of the wire, T_{av} – average temperature of the temperature rise.

$E = 2700 \cdot 10^{-5} \cdot 4 \cdot \sqrt{\frac{2 \cdot 400 \cdot 4}{10^{-10} \cdot 7.7^2 \cdot 10^{14}}}$ = 7.9 mJ. This is valuable amount of the energy to make the wire of the CBM magnet coil to be normal, as it is several orders more than in conventional superconducting magnets having wires with NbTi/Cu ratio about 1. So, one may conclude that the training of the coils during the first ramping up will take not much time, or it may not occur at all.

Uniform dissipation energy in one coil

The uniform dissipation of the stored energy in one coil is described in the TDR [1] that is according the current design of the CBM magnet. Heat exchange between the winding and the stainless steel case was not counted. In this case we have:

- E/M ratio is about 6.5 kJ/kg;
- coil temperature after such uniform quench will be about 90 K;
- resistance of one winding after such quench is about 4 Ohm;
- characteristic time of the current decay is about 10 s (L/R);
- the estimated voltage inside the winding, relating the case when a quench started inside the coils (non-uniform quench), is about 1.3 kV;
- the thickness of interlayer insulation is about 0.9 mm, assuming breaking voltage for insulation of 10 kV/mm^2 – among the lowest values, we have safety factor at least 9/1.3 = 7 for the breaking voltage.

Hot spot temperature estimation

After appearing of a hot spot causing a quench it will be the hottest place of the superconducting winding after the total current decay. Its temperature can be estimated according the following evaluation. Consider a part of the SC wire- Δl which becomes normal. Joule heat will go to increasing the temperature of the considering mass (m) of Δl length of the SC wire. The current goes only through the copper matrix which resistance is of three orders lower than resistance of the superconductor. In adiabatic condition the current going through it generates Joule heating:

$$R(T) \cdot I^2(t)dt = m \cdot C_p(T)dT$$

$$\rho(T)\frac{\Delta l}{S_{Cu}} \cdot I^2(t)dt = \Delta l \cdot S \cdot \gamma \cdot C_p(T)dT,$$

where I [A] – operating current ($I = J*S_{Cu}$), S_{Cu} – area of the copper matrix, J [A/m^2] – current density, γ [kg/m^3] – material density. It is assumed that the whole SC wire is heated, not copper matrix only. So, S is the area of the whole wire. For a quench analysis it is useful to have the following form of the integrated equation which will be used in the temperature estimations:

$$U(T) = \int_{4,2}^{T_{max}} \frac{\gamma C_p(T)dT}{\rho(T)} = \frac{S_{Cu}}{S} \cdot J_0^2(t) \cdot \Delta t,$$

where λ - SC/Cu ratio, Δt – integrated time of the current decay, j_0 – current density magnitude in the copper matrix at the beginning of a quench, $C_p(T)$ – mass heat capacity [J/kg], $\rho(T)$ – electrical resistance of the copper matrix. The U(T) integrated function is shown on the Fig. 25 below. The Δt time may be considered as sum of τ_0 and $\tau/2$, where $\tau/2$ is half of the characteristic time of the current decay. The τ_0 is time of the normal zone spreading without visible current decay that is at the beginning of the quench. The $\tau/2$ time relates to decaying current with an exponent coefficient of $\tau \sim L/R$.

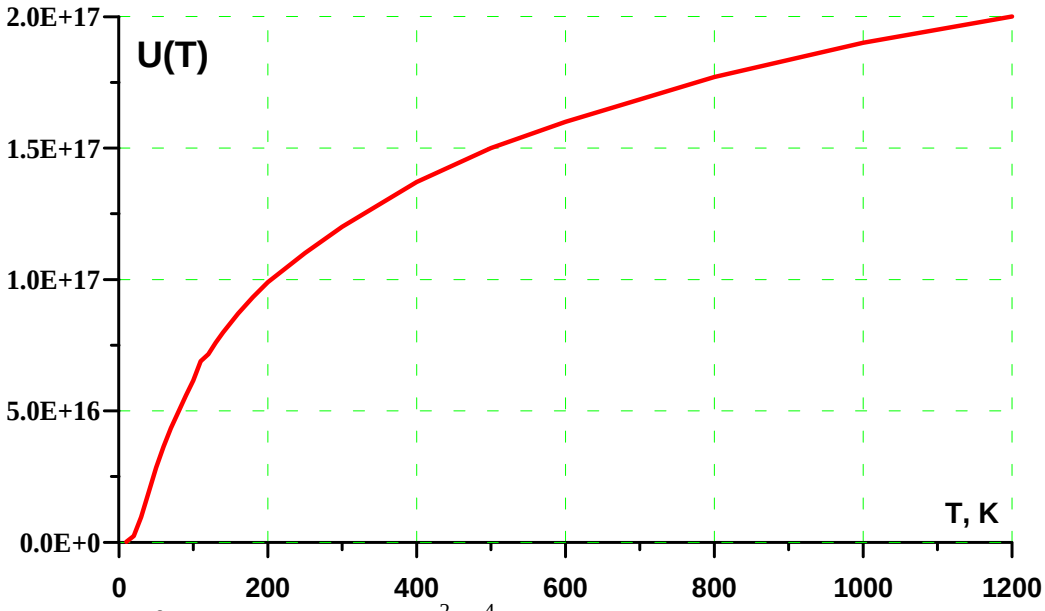

Fig. 25. The U(T) function in SI units (A^2/m^4*s).

So, at uniform quench at nominal current 686 A it will be:

$U(T) = \frac{S_{Cu}}{S} \cdot J_0^2(t) \cdot \Delta t = \frac{5.72}{6.23} \cdot \frac{686^2}{5.72^2} \cdot 10^{12} \cdot 5 = 6.5*10^{16}$ A^2/m^4*s. So, it gives the uniform temperature after a quench about 110 K. The winding insulation is not included in this estimation.

In order to estimate the hot spot temperature the τ_0 time should be estimated. Taking the results obtained below,

Taking τ_0 time as 3.5 s it will be 8.5 s for the Δt time, and U(T) = $1.1*10^{16}$ A^2/m^4*s, and the temperature in the hot spot will be not more than 210 K in this rough estimations.

Existence of the secondary circuits, ***described below***, reduces the amplitude of the current density by a factor of $\tau_1 / (\tau_1 + \tau_2)$, it will be as 10/11 = 0.9, so U(T) = $0.9^2*1.1*10^{16} = 9*10^{15}$ A^2/m^4*s, and the maximal temperature in the hot spot will be about 190 K.

Normal zone propagation velocities

The velocity of the normal zone propagation along the wire [M. Wilson] is

$v_a = \frac{J_e}{\rho C}\sqrt{\frac{L_o \cdot T_s}{T_c - T_s}}$, where J_e – engineering current density, ρC – heat capacity [$J/(m^3*K)$], L_0 = $2.45*10^{-8}$ $W*\Omega/K^2$, T_s – average temperature of heat generation, T_c – critical temperature of NbTi.

$v_a = \frac{7.7*10^7 \cdot 10^{-4}}{2700}\sqrt{\frac{2.45 \cdot 7}{9.6 - 7}}$ = 7.3 m/s, so it will take about 0.67 s for the normal zone to go around one turn of the coil.

The velocity of the normal zone across the wire was estimated in 2D model using ANSYS, as shown on the Fig. 26. The heat generation in the normal wire was set $2.2*10^6$ W/m^3, at was assumed that in the neighbor wire it was the same heat generation at the temperature of 7 K.

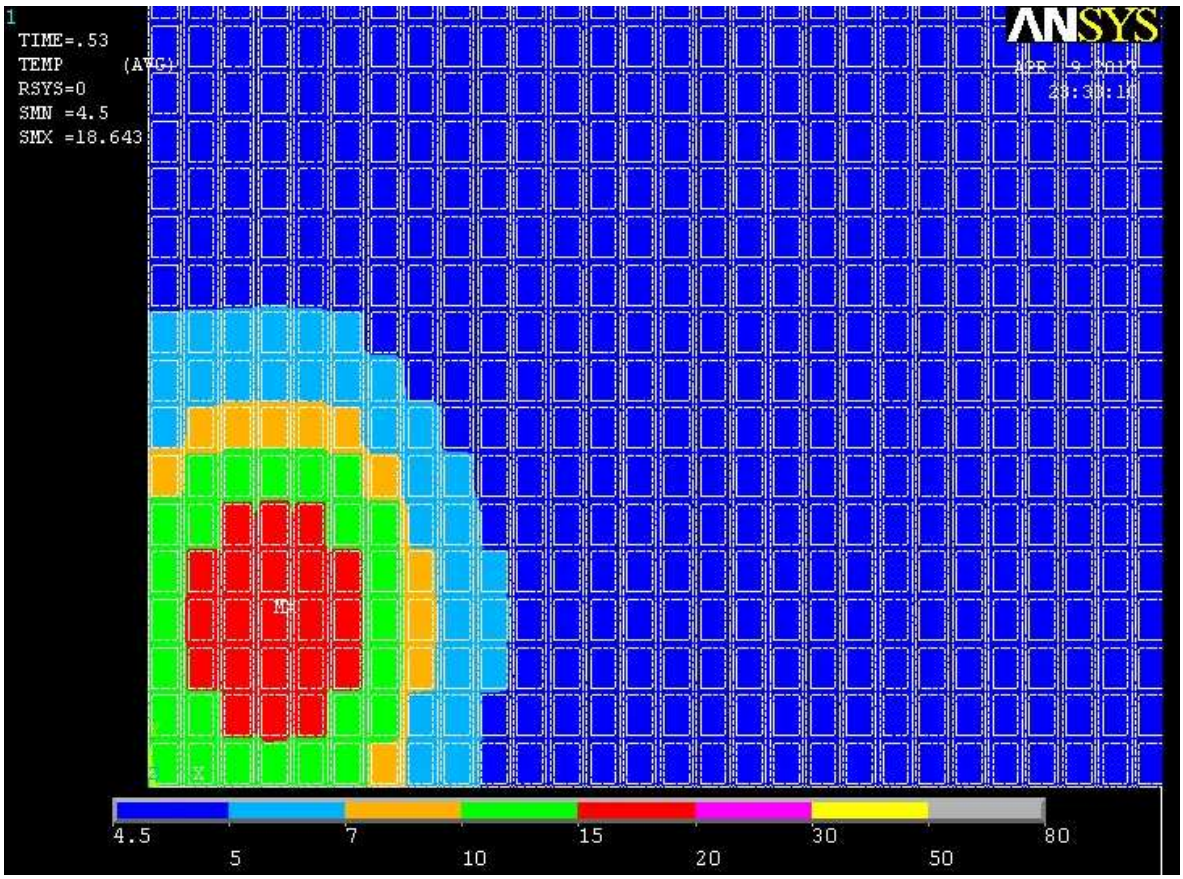

Fig. 26. Normal zone propagation in the winding in 2D calculations. Here time after start of the quench is 0.53 s, the quenched wire is in the center of the red zone and its maximal temperature is 18.6 K.

The velocity across the wire was about 0.05 m/s. This is low value, because typically such velocity has some 1-3% from the v_a value, as it mentioned in literature for convenient superconducting magnets. The reason is to high amount of the insulation between the layers of the winding. This velocity is also slightly faster for a direction along the layer. The maximal time for a normal zone going from the 1st layer to the 53rd is 0.159/0.05 = 3.2 s. So, the total τ_0 time will consists of half time of the normal zone distribution along the wire is ~ 0.3 s and of 3.2 s, - **τ_0 = 3.5 s**.

It is worth to note that if the normal zone starts to propagate in the 1st or 53rd layer, depending on the coil, the normal zone will reach the neighbor coil.

Effect of a Secondary circuit's protection

This method is described in literature [M. Wilson] and elsewhere. During a quench in all circuits in the magnet system eddy currents appear. They may significantly decrease the amplitude of the decaying current in the superconducting magnet and some part of the stored energy will be dissipated in them. The taper part of the iron yoke will work as that secondary circuit, and how much will be shown below.

The first circuit is the superconducting magnet, the second one is any circuit with low electrical resistance, Fig. 27. At the beginning the $I_1(t=0) = I_0$ and $I_2(t=0) = 0$.

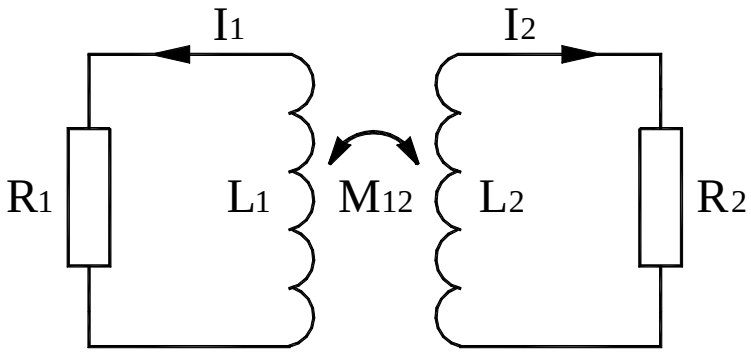

Fig. 27. Scheme of the coupled circuits.

The equations to be solved are:

$$I_1R_1 + L_1\frac{dI_1}{dt} + M\frac{dI_2}{dt} = 0;\ I_2R_2 + L_2\frac{dI_2}{dt} + M\frac{dI_1}{dt} = 0.$$

The result of the solving is [7]:

$$I_1 = \frac{I_0}{\tau_L - \tau_s}\left[(\tau_1 - \tau_s)\cdot\exp(-t/\tau_L) + (\tau_L - \tau_1)\cdot\exp(-t/\tau_s)\right],$$

$$I_2 = \frac{M\cdot I_0}{L_2(\tau_L - \tau_s)}\left[(\tau_2 + \tau_s)\cdot\exp(-t/\tau_L) - (\tau_2 + \tau_s)\cdot\exp(-t/\tau_s)\right],$$

where $\tau_1 = \frac{L_1}{R_1}$, $\tau_2 = \frac{L_2}{R_2}$, $\tau_L = \tau_1 + \tau_2$, $\tau_s = \frac{\varepsilon\cdot\tau_1\tau_2}{\tau_1 + \tau_2}$, $\varepsilon = 1 - \frac{M^2}{L_1L_2}$. L_1 and L_2 - inductances. R_1 – resistance of the superconducting magnet, R_2 – resistance of the secondary circuit. M_{12} – mutual inductance. The τ_L time is “long” time having sense of the total currents decay. The τ_s time is “short” time having sense of the current transition from primary circuit to the secondary one. If the value of τ_s is low, what happens at good coupling between the circuits, the amplitudes of the currents will be:

$I_1 = \frac{\tau_1}{\tau_1 + \tau_2}I_0$, and $I_2 = \frac{\tau_2}{\tau_1 + \tau_2}\frac{N_1}{N_2}I_0$, where N_1 and N_2 is the number of turns in the corresponding circuits (N_2 = 1 in our case).

The most important is that the value of τ_2 should be as large as possible in order to decrease the amplitude of I_1, what is seen in the results of the equations.

Estimation of τ_2 of the iron taper inside the coils

The τ_2 characteristic time of the current decay is evaluated as L/R ratio. Eddy currents go non-uniformly in such taper having increasing current density towards outer circumference.

The estimated inductance with ANSYS is about $7*10^{-7}$ H.

The estimated resistance at $\rho = 8.6*10^{-8}$ Ω*m at 273 K for iron is about $R = 6.4*10^{-7}$ Ω.

So, the characteristic time is about $\tau_2 \approx 1$ ***s*** for one taper. In our case we have two taper working independently, it means that the first equation will be written as: $I_1R_1 + L_1\frac{dI_1}{dt} + 2\cdot M\frac{dI_2}{dt} = 0$ and the coefficient ε in the short time will be higher: $\varepsilon = 1 - \frac{2\cdot M^2}{L_1L_2}$. It means that the current rise in the iron taper will be faster.

Component properties

Property	Stainless steel	GFRP material	Coils	Epoxy		
Thermal expansion coefficient, K^{-1}	$1.02\ 10^{-5}$	$1.2\ 10^{-5}$	$1.2\ 10^{-5}$	$1.2\ 10^{-5}$		
Shear modulus in xz plain, Pa	$7.5\ 10^{10}$	$4.0\ 10^{9}$	$1.9\ 10^{10}$	$4.0\ 10^{9}$		
Young modulus y direction, Pa	$2.0\ 10^{11}$	$1.8\ 10^{10}$	$4.1\ 10^{10}$	$9.0\ 10^{9}$		
Thermal expansion coefficient y direction, K^{-1}	$1.2\ 10^{-5}$	$1.0\ 10^{-5}$	$1.57\ 10^{-5}$	$6.0\ 10^{-5}$		
Thermal expansion coefficient xz plain, K^{-1}	$1.2\ 10^{-5}$	$1.6\ 10^{-5}$	$9.2\ 10^{-6}$	$1.6\ 10^{-5}$		
Young modulus xz direction, Pa	$2.0\ 10^{11}$	$2.2\ 10^{10}$	$8.6\ 10^{10}$	$1.8\ 10^{10}$		

Results of the quench estimation:

Maximal hot spot

Heat transition between the coil and the st steel case

Eddy current in the st steel case

Quench heater should be more than 8 cm of length

Point of discussion – thickness of the interlayer insulation, may it be decreased to 0.1 or 0.2 mm?

3.5 Quench protection system

4. Cryogenics of the CBM detector

4.1 Cryogenic diagram

The cryogenics diagram of the CBM magnet is presented on the Fig. 28. The cryogenics of the CBM detector consists of the Branch Box (BB), the Feed Box (FB), the cryostat of the CBM detector and the cryogenic transfer lines. The length of the transfer lines between the BB and the FB is about 30 m.

For the transfer line the most tubes were chosen to be DN15 STD, so OD = 21.34 mm, ID = 15.8 mm.

The parameters of the cryogenic valves are listed in the Table 7. The valves are of PN25 type – nominal pressure of 25 bar, they should have a Cu flange for a heat load interception along its stem.

The parameters of the valves are estimated at the following conditions:

- maximal heat loads for the CBM detector 60 W at 4.5 K and 3 bar, so G = 2.8 g/s = 10 kg/h;
and 190 W at 50 K and 18 bar, so G = 1.8 g/s = 6.5 kg/h;
- maximal heat loads for the HADES detector 150 W at 4.3 K G = 6.9 g/s = 25 kg/h;
and 400 W at 50 K and 3 bar, so G = 3.8 g/s = 13.6 kg/h.

(The mass rate G was estimated via enthalpy difference as Q/Δh.)

Valve coefficient for the control valves $K_V = \frac{G}{514}\sqrt{\frac{T_1}{\rho_g \cdot \Delta p \cdot p_1}}$, and for JT valves is: $K_V = \frac{G}{257 \cdot p_1}\sqrt{\frac{T_1}{\rho_g}}$, where G – mass flow rate [kg/h], p_1 and T_1 – upstream pressure [bar] and temperature [K], Δp – pressure difference between the valves, taken as 0.01 bar; ρ_g – gas density at normal conditions [kg/m^3].

Table 7 Cryogenic valves list.

Valve	Valve purpose, Couplings	Kv, max	Kvs	DN, mm	G_{op}, g/s	Pop, bar	Top, K	Position without electricity
QN1	Open at all operating modes	0.14		15		2.5→1.2	70	Open
QN2		0.051		15		1.3	6	
QN3		1.32		15		2	70	
QN4		0.071		15		2	4.5	
QN5		0.052		15		3	4.6	
QN6	Reduction to 3 bar	0.010		15		18→3	50	Closed
QN7		0.053		15		18	50	
QN8		0.021		15		3	4.6	
QN9		0.081		15		1.3	4.5	
QN10		0.77		15		17	70	
QN11		1.92		15		17	85	
QN12		0.11		15		1.3	5	
QN13		0.053		15		18	50	
QN14		0.076		15		17	70	
QN15		0.072		15		1.3	4.5	
QN16		0.053		15		18	50	
QN17		0.022		15		3	4.6	
QN18	JT	0.022		15		3	4.5	
QN19		0.39		15		2	300	

General approaches for the cryogenic system are:

- the radiation shields of all cryogenic subsystems should be cooled by return line of 55-60 K helium;
- the Branch Box may has installed vacuum pumps installed;
- vacuum behavior of the systems after a quench as in CBM and HADES detectors or warming up in one detector at operation of another should be taken into account;

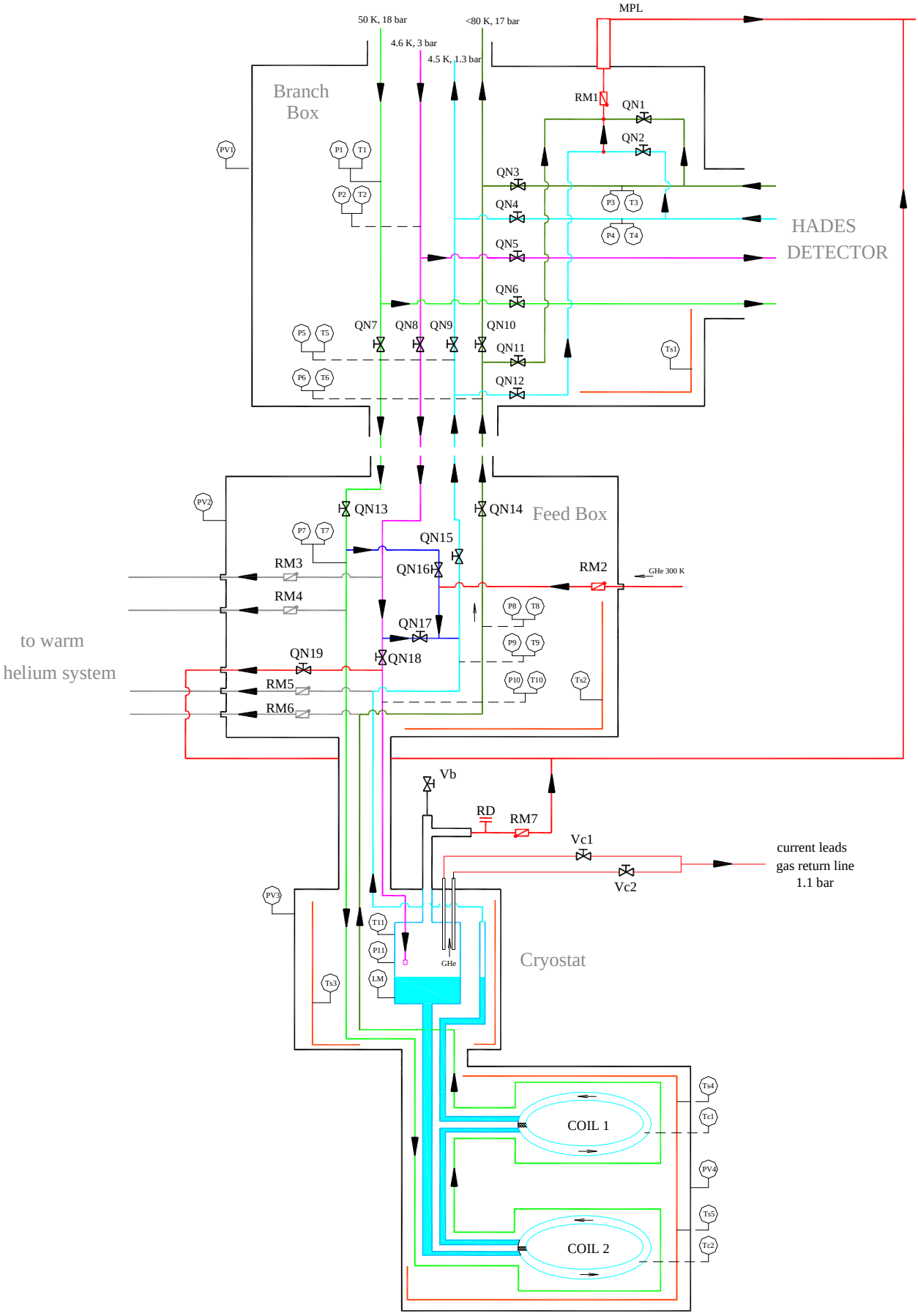

Fig. 28. General view of the CBM detector cryogenic diagram.

The designations on the diagram of the Fig. 28 are: QN – control valves, RM – check valves, P – pressure gauge, T – temperature sensor, PV – vacuum gauge.

4.2 Design of the Feed Box

The design of the Feed Box is shown on the . The cryogenic diagram of the Feed Box is shown on the Fig. 28. The Feed Box should perform all cryogenic operations of the CBM magnet such as cooling down, routine operation at 4.5 K, warming up and quench recovery.

The control valves will give a major part of heat in-leaks, the interception at 60 K temperature should be foreseen at procurement stage of work.

Items for discussion

It is demanded to have warm helium purge system and warm helium line for warming up the magnet. It is not clear why the purging can't be performed during installation of the system when the helium lines can be vacuum pumped. After this the cryogenic system can be purged by helium from the cryoplant.

For warming up of the magnet may be a heat exchanger installed between QN13 and QN16 valves will be simpler to warm 50 K to desired temperature. Power of the heat exchanger may be around 1 kW.

4.3 Design of the Branch Box and the transfer line

The destination of the Branch Box is to supply He gases the CBM and the HADES detectors. All cryogenic operations of these detectors should be performed independently. So, the scheme and the placement of the cryogenic valves in the Branch Box should have symmetry, as it is shown on the cryogenic diagram, Fig. 28. The helium goes from the local cryoplant and after the Branch Box it may go ever to CBM detector ever to the HADES. The return lines of the Branch Box will have sensors of temperature and pressure for controlling parameters of helium. In case of improper parameters of helium the return gas will go to the multipurpose line.

In the current design the vacuum volume of the CBM cryogenics and the HADES cryogenics is common. In case of a quench in any system the other may not see the vacuum deterioration due to large length of the transfer lines. But during warming up of the CBM cryogenics, 4.6 K lines, all condensed gases accumulated for many months of work may go to the HADES cryogenics.

4.4 Estimations of pressure drops and heat transfer

These estimations will determine a diameter of a pipe and a mass flow rate for the transfer pipes from the Branch Box to the cryostat and will evaluate the needed mass flow rate for the heat transfer. The pressure drop along the transfer line should be much less than 0.1 bar at ordinary operation of the CBM magnet.

Pressure drop of isothermal gas along a pipe can be evaluated by the following formula:

$\Delta p = \xi \frac{v^2 \rho}{2} \cdot \frac{L}{d}$, where ρ - density, v – velocity, L and d – length and diameter of a pipe, ξ - friction coefficient. Addition pressure drop appears due to acceleration of gas heated along a pipe – not considered here.

With a mass flow rate $G = v*\rho*d^2*\pi/4$ it will be more convenient:

$$\Delta p = \xi \frac{8G^2}{\pi^2 \rho} \cdot \frac{L}{d^5}.$$

Reynolds number $Re = \frac{4G}{\pi d \eta}$ determines the flow mode, where η - viscosity [Pa*s].

At turbulent flow, when Re = $2.3*10^3 \div 10^5$, the friction coefficient is calculated as $\xi = \frac{0.316}{Re^{0.25}}$.

The input parameters of the pipe are inner diameter ID = 15.8 mm and the length of the pipe L = 120 m. The length of the pipe includes the length itself and additional length from the valves, and bellows parts. The parameters of helium at various temperature and pressure are listed in the Table 8 that will be used in the following estimations.

For the 4.6 K helium lines at G = $1.7*10^{-3}$ kg/s we have:

$$Re = \frac{4G}{\pi d \eta} = \frac{4 \cdot 1.7 \cdot 10^{-3}}{\pi \cdot 0.0158 \cdot 3.4 \cdot 10^{-6}} = 40000$$ – turbulent flow.

Friction coefficient $\xi = \frac{0.316}{Re^{0.25}} = 0.022$.

Pressure drop: $\Delta p = \xi \frac{8G^2}{\pi^2 \rho} \cdot \frac{L}{d^5} = 0.022 \cdot \frac{8 \cdot 2.89 \cdot 10^{-6}}{\pi^2 \cdot 128} \cdot \frac{120}{0.0158^5} = 49$ Pa = 0.00049 bar.

In the ordinary operation the pressure drop along the transfer lines is very low.

For the 50 K helium lines at G = $1.8*10^{-3}$ kg/s we have:

$$Re = \frac{4G}{\pi d \eta} = \frac{4 \cdot 1.8 \cdot 10^{-3}}{\pi \cdot 0.0158 \cdot 7.4 \cdot 10^{-6}} = 20000$$ – turbulent flow.

Friction coefficient $\xi = \frac{0.316}{Re^{0.25}} = 0.027$.

Pressure drop: $\Delta p = \xi \frac{8G^2}{\pi^2 \rho} \cdot \frac{L}{d^5} = 0.027 \cdot \frac{8 \cdot 3.24 \cdot 10^{-6}}{\pi^2 \cdot 14} \cdot \frac{120}{0.0158^5} = 617$ Pa = 0.006 bar

In the ordinary operation the pressure drop along the transfer lines is also very low.

Heat transfer between helium and tubes for cooling

The return helium at 50-70 K of temperature should cool the heat in leaks presented in the Table 4 and Table 6. The temperature differences should be estimated between the helium and the cooling tubes of radiation shields in all components of the CBM magnet cryogenics.

The heat transfer between the helium and the pipe wall is estimated as:

Q = $\alpha S*\Delta T$, where α - heat transfer coefficient, S – heat transfer surface, ΔT – temperature difference between helium and a pipe wall.

The heat transfer coefficient is estimated as $\alpha = \frac{\lambda \cdot Nu}{d}$, where λ - thermo conductivity coefficient of helium, Nu – Nusselt number, d – inner diameter of a tube.

The reduced heat transfer coefficient may be taken into account if tube wall is thick and has low thermal conductivity (w – wall parameters):

$\frac{1}{\alpha_r} = \frac{1}{\alpha} + \frac{h_w}{\lambda_w}$, where h_w – wall thickness.

For turbulent flow Nusselt number is estimated as: Nu = $0.023*Re^{0.8}Pr^{0.33}$, where $Pr = \frac{\eta c_p}{\lambda}$ - Prandtl number, where c_p – heat capacity.

For 60 K helium Nu = 56, so $\alpha = \frac{0.055 \cdot 56}{0.0158} = 195$ W/(m^2*K).

Heat load for one coil from support struts and the radiation shield is about Q = 25 W. The cooling tube going around the radiation shield has cooling surface S = πd*L = 3.14*0.0158*5 = 0.25 m^2. So, the temperature difference between helium and tube wall will be:

$\Delta T = Q/\alpha S = 25/(195*0.25) = 0.5$ K.

The cooling helium will be heated, its temperature can be estimated as:

$Q = G*c_p*\Delta T_h$, then $\Delta T_h = Q/(G* c_p) = 25/(1.8*5.3) = 2.6$ K. So, helium entering the lower coil at 50 K will go to the upper coil at temperature 52.6 K that is acceptable.

Table 8. Parameters of helium at given T and p.

T, K	**p, MPa**	**ρ, kg/m^3**	**λ ,W/(m*K)**	**10^{-6} μ, Pa*s**	**h, kJ/(kg)**	**Pr**
4.6	0.1	13.6	0.009	1.3	33.5	1.15
4.6	0.2	121.5	0.02	3.2	11.8	
4.6	0.3	127.8	0.02	3.4	11.9	
4.5	0.1	14.2	0.009	1.25	32.7	1.15
4.5	0.2	124.2	0.019	3.2	11.2	
4.5	0.3	129.8	0.02	3.4	11.4	
50	1.0	9.5	0.048	6.5	266.1	
50	1.5	14.0	0.049	6.6	275.3	
50	2.0	18.4	0.05	6.7	275.8	
60	1.0	7.9	0.054	7.3	318.5	
60	1.5	11.7	0.055	7.35	328.3	
60	2.0	15.4	0.055	7.4	329.1	0.69
70	0.1	0.7	0.058	7.83	369.0	
70	1.0	6.8	0.059	7.0	371.0	
70	1.5	10.0	0.060	8.0	380.9	
70	2.0	13.3	0.061	8.1	381.9	
80	1.0	6.0	0.065	8.7	423.2	
80	1.5	8.8	0.065	8.7	433.4	
80	2.0	11.7	0.066	8.8	434.5	
100	0.1	0.48	0.074	9.8	534.3	0.67
100	0.2	0.96	0.074	9.8	534.5	
100	1.5	7.1	0.075	10.0	537.8	
100	2.0	9.4	0.076	10.0	539.1	
140	0.1	0.34	0.093	11.9	742.1	
140	0.2	0.69	0.093	11.9	743.3	
140	1.5	5.1	0.094	12.1	746.0	
140	2.0	6.7	0.094	12.1	747.5	
200	0.1	0.24	0.118	15.1	1053.7	0.67
200	0.2	0.48	0.118	15.1	1054.0	
200	1.5	3.57	0.119	15.3	1057.8	
200	2.0	4.75	0.120	15.3	1059.3	
240	0.1	0.2	0.134	17.1	1261.4	
240	0.2	0.4	0.134	17.1	1261.7	
240	1.5	3.0	0.135	17.2	1265.5	
240	2.0	4.0	0.135	17.2	1267.0	
273	0.1	0.175	0.146	18.6	1423.2	
273	0.2	0.35	0.146	18.7	1423.6	

4.5 Operation modes of the CBM magnet cryogenics

The cryogenic system of the CBM magnet should work at the following operating conditions:
- cooling down the system during two weeks;
- ordinary operation of cooled magnet at 4.5 K;
- warming up of the magnet for demanded time;
- quench recovery.

Cooling down of the system

The biggest gold mass of the system is the superconducting magnet having about 3.6 tonnes and the internal energy is about 320 MJ. The rest cold components of the cryogenic system will be cooled down much faster and may be not considered here. Three stages of the cooling down will be proposed:
- first stage – the magnet is cooled to ~ 200 K;
- second stage – the magnet is cooled to ~ 80 K;
- third stage – the magnet is cooled to 4.5 K – operating conditions.

First stage – cooling down to ~ 200 K

Before cooling down, the system should have vacuum in the range $10^{-2} \div 10^{-3}$ Pa. The vacuum pump will be attached by the cryostat where it will have effective pumping capacity not more than 500 l/s.

For cooling a magnet from room temperature to ~ 200 K one needs to take off about 50% of the internal energy. In our case it will be 160 MJ and the cooling time is 48 hours. So, the desired cooling capacity is 930 W.

It is assumed in the TDR that the cooling rate should be about 2 K/hour, the high cooling rate may lead to high mechanical stress inside the superconducting structure. From another hand, if a magnet is cooled uniformly this rate may be higher. If firstly the radiation shields of the coils will be cooled down to about 200 K the heat transfer via radiation and support struts conduction will take place. The effect of these factors can be estimated as follows.

The cooling by the radiation shields is

$Q = \varepsilon S \sigma (T^4 - 200^4)$ where ε - total emissivity was taken as 0.06, S – surface area of the two LHe cases is 8.5 m^2, T – magnet temperature.

The results are Q = 85 W for T = 260 K, and Q = 21 W for T = 220 K.

The cooling by the support struts via G-10 elements is estimated as:

$Q = \lambda S^* \Delta T / L$, where λ - thermal conductivity was taken as 0.8 W/(m*K), S – cross-section area of one support is 9.1^*10^{-3} m^2, ΔT – temperature difference was taken as 100 K, L – length is about 0.16 m.

The result is Q = 55 W for ΔT = 100 K on the length of the support struts.

So, the cooling down the shields only will give cooling capacity from ~150 W at the beginning to about 50 W in the first stage.

BINP proposes to control the cooling process by measuring the temperature difference in the winding structure in order to be less than 10 K during the cooling down process. This is direct way for controlling the safe conditions during the cooling down process. The cooling diagram is shown on the Fig. 29.

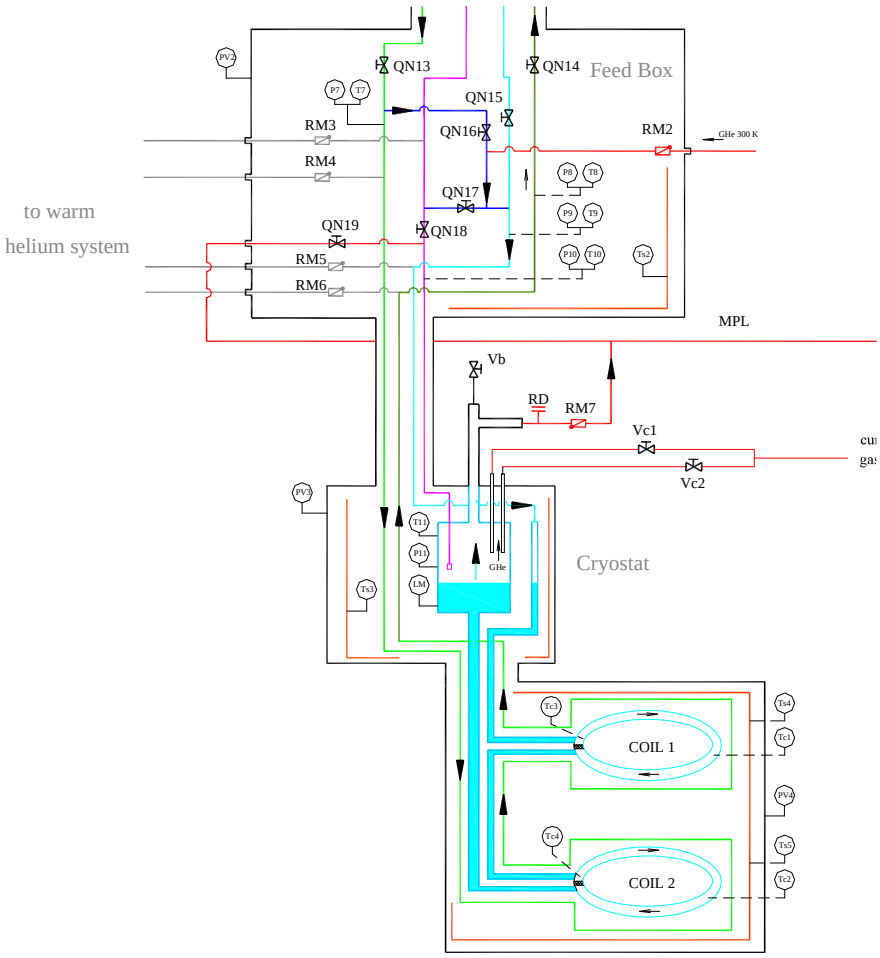

Fig. 29. The diagram of the cooling down procedure of the first and the second stages. The arrows show the helium running helium.

The coils are cooled by helium from 50 K line. The flow is divided between shields and coils by the QN16 valve. The mass flow rate of 0.9 g/s value or lower is enough in this stage.

The cooling helium has large cooling capacity due to high heat transfer coefficient, big cooling surface ~ 1.5 m^2 for every coil, even taking into account reduced heat transfer coefficient due to presence of G-10 around the coil.

The cooling is controlled by thermal sensors which are shown on the Fig. 29. If the temperature difference became more than 10 K the helium flow may be decreased by closing the QN16 valve. Temperature difference in solid body is dissipated with characteristic time as:

$t = \frac{C_v \cdot \langle L \rangle^2}{\lambda \cdot \pi^2}$, where C_v – volumetric heat capacity, λ - thermal conductivity, L – characteristic length of temperature difference. In the first stage of cooling down this time is about one hour.

Second stage – the magnet is cooled to ~ 80 K

The cooling diagram in this stage is the same. In the controlling process one needs to increase the mass flow if the cooling down rate becomes too slow due to decreasing of temperature difference between the coil and the cooling helium.

Third stage – the magnet is cooled to 4.5 K

In this stage the line of 4.6 K helium will be used. In is assumed that the line itself already has a temperature not high than 60 K as it was surrounded by operating 50 K lines. The cooling starts with closing QN16 valve and opening QN17 valve.

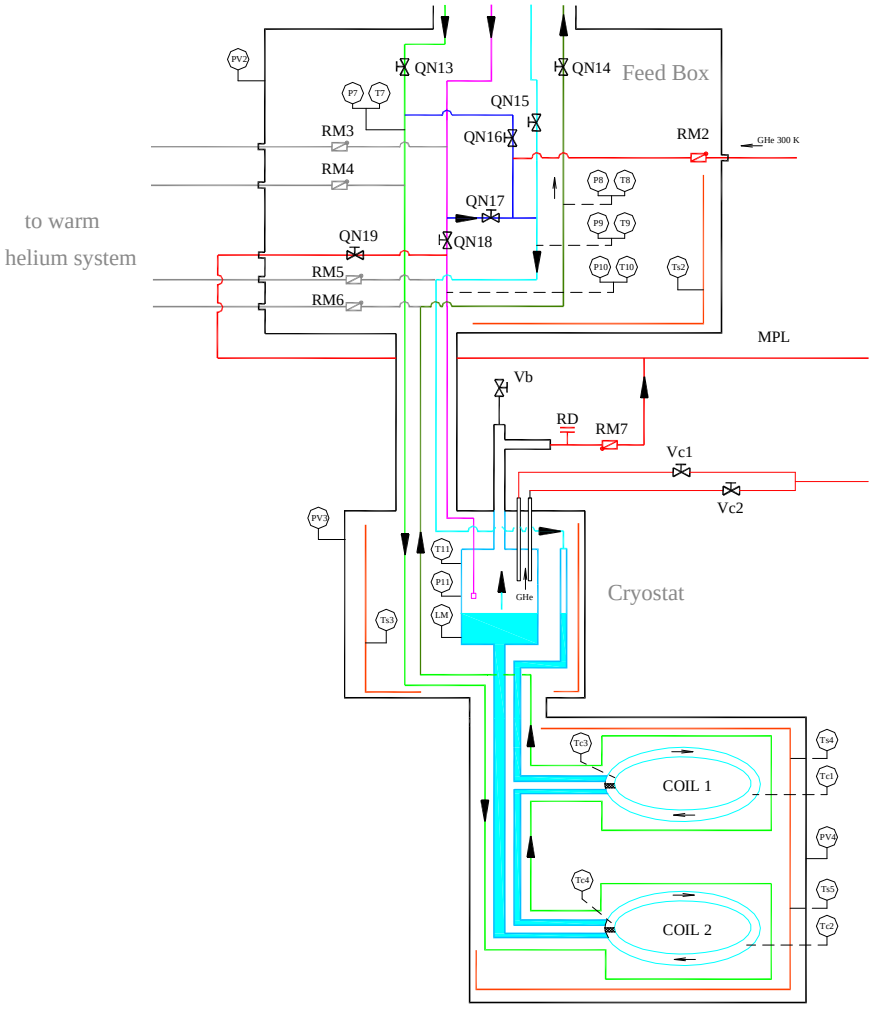

Fig. 30. The diagram of the cooling down procedure of the third stage.

At the end of the cooling when liquid helium starts accumulating on the lower coil one may close QN17 valve and open QN15 and QN18 valves, then liquid helium will fill the cryostat. The moment of liquid helium accumulation in the low coil may be detected by pressure drop in the cryostat on P11 manometer.

Total cooling down time will be about 8 days.

Ordinary operation of the cooled magnet at 4.5 K

In the ordinary operation of the cryogenic system the helium flows will be as shown on the Fig. 28. Some part of gaseous helium will go through the current leads, it flow will be controlled by a heater installed in the cryostat.

The liquid helium level will be measured by installed LHe level meter.

One of the possible scenarios of LHe level controlling is to operate at insufficient flow of helium by controlling of QN8 valve, i.e. 1.5 g/s instead of demanded 1.7 g/s of flow rate. When the LHe level becomes too low then the QN18 will be opened to supply 1.8 g/s rate until demanded level of helium in the cryostat.

Warming up of the magnet for demanded time

For accelerated warming up the 300 K line of helium is installed to the Feed Box. This process will be conducted on the same principle as in the cooling down in the first and the second stages. The supply of 50 K helium should by shut. After increasing the lowest temperature in the cryogenic system beyond 27-28 K the insulated vacuum pressure will be increased rapidly.

Quench recovery

If quench had occurred then the QN8 and QN9 valves should be closed. The rising pressure in the cryostat will open RM7 valve to the multipurpose line. Liquid helium in the cryostat will not go down to the coils. The highest pressure in the system will be not more than 3 bar due to little amount of stored liquid helium in the system.

In the worse case of quench, stored energy fully dissipated in one coil – this coil after a quench will be slowly cooled from ~ 90 K to ~ 50 K due to heat transfer between the winding and the heavy coil case. After this the cooling down procedure will go as in the third stage of cooling down the magnet.

4.6 Safety analysis

Very high pressure may be in the cryostat in case of a quench in the magnet or any break of insulating vacuum when air or even helium can leak inside the vacuum volume. This pressure can be estimated as follows. It is assumed that the cryostat is equipped with relief valve allowing helium to go into the multipurpose line.

Formula for pressure buildup in the cryostat:

$\Delta p = \xi \frac{8G^2}{\pi^2 \rho \cdot Y^2} \cdot \frac{L}{d^5}$, where Y – expansion correction coefficient, about 0.8; the rest parameters are the same as for the pressure drop.

The mass rate G is determined by external heat flow to the helium in the LHe case. Typical heat transfer coefficient is about 10^3 W/(m^2*K) that can be found in literature. It may be reduced by a factor of 2 because heat transfer going through G-10 insulation (quench case) or thick wall of stainless steel (vacuum break). So, the heat flux to helium can be q = 5000 W/m^2 at temperature difference about 10 K – film boiling. The heat transfer surface is about 1.5 m^2 in one coil case. So, total heating power can be about Q = 5000*3 = 15 kW. The mass rate is determined as G = Q/Δh, where Δh – latent heat, about 21 J/g. The length of the pipe is about 3 m, diameter was chosen 0.03 m. G = 0.714 kg/s.

$\Delta p = 0.03 \frac{8 \cdot 0.714^2}{\pi^2 14 \cdot 0.64} \cdot \frac{3}{0.03^5}$ = 1.7*10^5 Pa = **1.7 bar**. This is maximal overpressure in the cryostat during a quench at condition that helium goes out through the cryostat neck to the multipurpose line.

It is worth to note that LHe volume in both coils will be not more 30 l, i.e. total mass is 30*124 = 3.7 kg. It means that at given mass rate all liquid helium will go out after 5 s. This time is comparable with the current decay during a quench; it means that helium will start to go out at lower pressure.

The estimated mass flow rate is by a factor of 400 larger than the rate supplied from the cryoplant. The control valves may be closed during several seconds, no problems here seen.

Thermal oscillation may happen in the cryogenic system at various stages of operation. The simple thermal oscillations criteria can be used in designing the system, see Fig. 31.

Characteristic radius is calculated as: $R^*_c = r_0 \cdot \left(\frac{a}{\nu \cdot L} \right)^{1/2}$, where r_0 - tube radius, a - acoustic velocity, m/s, ν - kinematic viscosity, L - length of the pie.

$a = (\gamma \cdot R \cdot \bar{T})^{1/2} = (1.67 \cdot 2078 \cdot 20)^{1/2} = 263.4$ m/s for helium.

$\nu = \eta / \rho$

Another parameter is $\alpha = \frac{T_h}{T_c}$ - ration of warm end of a pipe to cold end of the pipe.

The stability region is at low values of given parameters $R^*_c < 8$ and $\alpha < 6$.

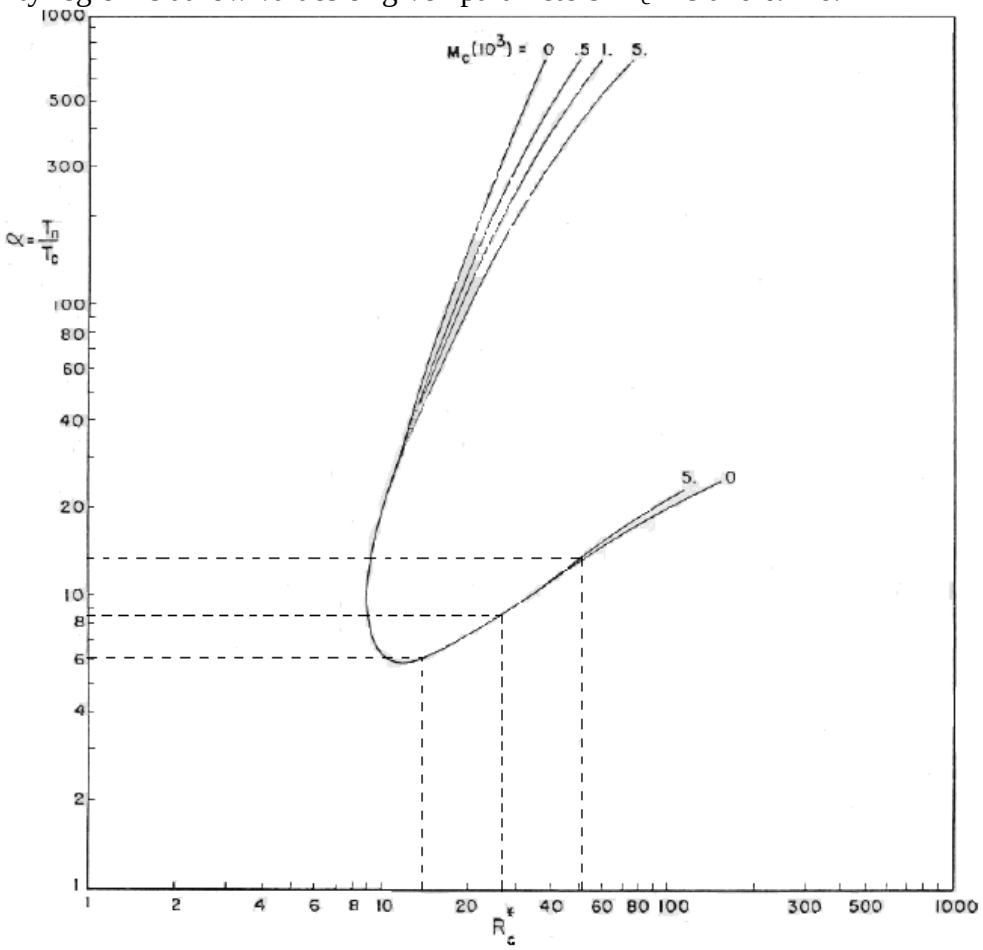

Fig. 31. The graph for the thermal oscillations criteria taken from [J.A. Liburdy].

This criteria shows that thermal oscillations will mostly occur during cooling down of the cryogenic system.

5. BINP tests of the CBM magnet (FAT)

The BINP does not have such cryogenic station to provide helium with parameters as of the CBM magnet. Currently it proposed to cool the CBM magnet with liquid helium directly into the cryostat and the radiation shields will be cooled by liquid nitrogen. In this case heat loads to the magnet will be increased.

Quench heaters for quench demonstration.

6. References

1. Collaboration Contract CBM-Magnet BINP Annex3 - Technical specifications, 2016.
2. Technical design report
3. M. Wilson, Superconducting magnets
4. Y. Iwasa, Case studies in superconductivity
5. Thermodynamical properties of helium, Sychev V.V. et al, 1984.
6. J.A. Liburdy, J.L. Wofford «Acoustic oscillation phenomena in low-velocity steady flow with heating», Advances in Cryogenic Engineering, 1980, Vol. 25, p. 528.

7. M.A. Green “Quench back in thin superconducting solenoid magnets”. Cryogenics, 1984, Vol. 24, n. 1, p. 3, *and* M.A. Green “The role of quench back in quench protection of a superconducting solenoid”. Cryogenics, 1984, Vol. 24, n. 12, p. 659.

8. Cryogenic data handbook, 1980.

9. J. Weisend Handbook of cryogenic engineering, 1998.